the plant journal

SEB SOCIETY FOR EXPERIMENTAL BIOLOGY

The Plant Journal (2022) **111,** 231–249 doi: 10.1111/tpj.15789

Knock-down of phosphoenolpyruvate carboxylase 3 negatively impacts growth, productivity, and responses to salt stress in sorghum (*Sorghum bicolor* L.)

Clara de la Osa[1] , Jesús Pérez-López[1] , Ana-Belén Feria[1] , Guillermo Baena[1] , Daniel Marino[2,3] , Inmaculada Coleto[2] , Francisco Pérez-Montaño[4] , Jacinto Gandullo[1] , Cristina Echevarría[1] , Sofía García-Mauriño[1] and José A. Monreal[1,*]

[1]*Departamento de Biología Vegetal y Ecología, Facultad de Biología, Universidad de Sevilla, Sevilla, Spain,*

[2]*Departamento de Biología Vegetal y Ecología, Facultad de Ciencia y Tecnología, Universidad del País Vasco (UPV/EHU), Leioa, Spain,*

[3]*Ikerbasque, Basque Foundation for Science, Bilbao, Spain, and*

[4]*Departamento de Microbiología, Facultad de Biología, Universidad de Sevilla, Spain*

Received 11 November 2021; revised 21 April 2022; accepted 25 April 2022; published online 30 April 2022.
*For correspondence (e-mail monreal@us.es).

SUMMARY

Phosphoenolpyruvate carboxylase (PEPC) is a carboxylating enzyme with important roles in plant metabolism. Most studies in C_4 plants have focused on photosynthetic PEPC, but less is known about non-photosynthetic PEPC isozymes, especially with respect to their physiological functions. In this work, we analyzed the precise roles of the sorghum (*Sorghum bicolor*) PPC3 isozyme by the use of knock-down lines with the Sb*PPC3* gene silenced (*Ppc3* lines). *Ppc3* plants showed reduced stomatal conductance and plant size, a delay in flowering time, and reduced seed production. In addition, silenced plants accumulated stress indicators such as Asn, citrate, malate, and sucrose in roots and showed higher citrate synthase activity, even in control conditions. Salinity further affected stomatal conductance and yield and had a deeper impact on central metabolism in silenced plants compared to wild type, more notably in roots, with *Ppc3* plants showing higher nitrate reductase and NADH-glutamate synthase activity in roots and the accumulation of molecules with a higher N/C ratio. Taken together, our results show that although SbPPC3 is predominantly a root protein, its absence causes deep changes in plant physiology and metabolism in roots and leaves, negatively affecting maximal stomatal opening, growth, productivity, and stress responses in sorghum plants. The consequences of Sb*PPC3* silencing suggest that this protein, and maybe orthologs in other plants, could be an important target to improve plant growth, productivity, and resistance to salt stress and other stresses where non-photosynthetic PEPCs may be implicated.

Keywords: central metabolism, phosphoenolpyruvate carboxylase, productivity, RNA interference, salt stress, stomata, *Sorghum bicolor*.

INTRODUCTION

Sorghum (*Sorghum bicolor*) is a diploid (2n = 20) C_4 crop belonging to the Poaceae family, with a relatively small genome (730 Mb) (Paterson et al., 2009). Sorghum has high photosynthetic efficiency and is considered to be tolerant to abiotic stresses, characteristics placing sorghum among the top five of the most important cereal crops feeding the world (Zhao & Dahlberg, 2019). Sorghum is a staple crop for over 500 million people in many developing countries, mainly in Africa and Asia, and is used for human food, livestock feed, renewable industrial materials, and biofuels. All these characteristics make sorghum a good choice as a model plant for studying C_4 photosynthesis or stress resistance. Although sorghum is more recalcitrant than other crops to *Agrobacterium*-mediated transformation, in the last years many improvements have been made and efficient protocols for transformation are now available and more examples of transgenic sorghum plants can be found in the literature (Do et al., 2016 and references therein).

Phosphoenolpyruvate carboxylase (PEPC; EC 4.1.1.31) is a cytosolic enzyme catalyzing the irreversible β-carboxylation of phosphoenolpyruvate (PEP), using bicarbonate as substrate, to yield oxaloacetate (OAA) and inorganic phosphate (Chollet et al., 1996). PEPC has been extensively studied in C_4 and CAM plants, where it carries

out the initial carboxylation of atmospheric CO_2. An *Amaranthus edulis* C_4 PEPC mutant needs elevated CO_2 levels to grow (Dever et al., 1995) and shows reduced germination due to reduced ATP content in seeds (Álvarez et al., 2011). In the CAM species *Kalanchoë laxiflora*, silencing of photosynthetic the *PPC1* gene impairs dark CO_2 fixation and perturbs the functioning of the circadian clock and the dark-opening of stomata (Boxall et al., 2020). In C_4 plants, OAA can be either reduced to malate by NADP-malate dehydrogenase (NADP-MDH) in the mesophyll chloroplast or converted to aspartate by aspartate aminotransferase (AAT) in the cytosol and transported to the bundle sheath cells (Kanai & Edwards, 1999). However, PEPC also participates in other non-photosynthetic metabolic processes where malate or aspartate may have a role, such as C/N interactions and anaplerotic flux, stomatal opening control, root excretion, seed development and germination, and many others (O'Leary et al., 2011).

In sorghum, PEPC is represented by a multigene family with six members (Sb*PPC1–6*) (Paterson et al., 2009), with each displaying different patterns of expression and location. SbPPC1 is the isozyme participating in C_4 photosynthesis and the major PEPC protein in leaves (Shenton et al., 2006), with similar protein levels to that of Rubisco. SbPPC2–5 are C_3-type PEPCs carrying out the non-photosynthetic functions described above, although the specific contribution of each isozyme remains mostly unknown. SbPPC2 is considered to be a housekeeping protein, with similar expression levels in all tissues (Shenton et al., 2006). SbPPC3 is the most abundant PEPC isozyme in seeds (Ruiz-Ballesta et al., 2016) and roots (Arias-Baldrich et al., 2017). SbPPC4 seems to participate during early seed development (Ruiz-Ballesta et al., 2016), and SbPPC5 is of unknown function and almost absent in all tissues analyzed. SbPPC1–5 are referred to as plant-type PEPCs (PTPCs), in contrast to SbPPC6, which is referred to as a bacterial-type PEPC (BTPC). PTPCs typically assemble *in vivo* as Class-1 PEPC homotetramers (O'Leary et al., 2011). The main difference between PTPCs and BTPCs is that BTPCs are much larger polypeptides owing to an intrinsically disordered domain (approximately 10 kDa) not found in PTPCs. This region mediates the interaction of BTPCs with PTPCs resulting in the formation of a novel, allosterically desensitized, and mitochondrial envelope-associating Class-2 PEPC complex (O'Leary et al., 2009; Park et al., 2012).

PEPC activity is regulated at many levels in plant cells. Sugar phosphates, primarily glucose 6-phosphate (glucose 6-P), act as allosteric activators, whereas the downstream products malate and aspartate act as allosteric inhibitors (Chollet et al., 1996). Reversible phosphorylation of PTPCs changes the kinetic properties of the enzymes by increasing their maximal reaction rate, their affinity for PEP, and their activation by glucose 6-P and decreasing the inhibition of the enzyme by malate (Echevarría et al., 1994; Takahashi-Terada et al., 2005). PEPC is phosphorylated by a dedicated Ca^{2+}-independent Ser/Thr kinase known as PEPC kinase (PPCK) (Echevarría & Vidal, 2003). In addition, sorghum PEPCs may be regulated by other post-translational modifications (PTMs) such as mono-ubiquitination (Ruiz-Ballesta et al., 2014), *S*-nitrosylation, and carbonylation (Baena et al., 2017) or binding to anionic phospholipids (Gandullo et al., 2019; Monreal et al., 2010), altering the exposition of its C-terminal end (Gandullo et al., 2021), modulating even further its activity and/or stability and adding more complexity to the study of PEPC regulation *in vivo*.

Soil salinity, mainly in the form of NaCl, is a major concern for agriculture worldwide, with more than 20% of total cultivated land salinized, and this area is expanding constantly (Munns & Tester, 2008). Salt stress reduces water uptake by the plants, causing osmotic stress, and generates ionic stress due to the accumulation of sodium and chloride ions in tissues (Lamers et al., 2020). These ionic and osmotic stresses restrain photosynthesis and metabolism and induce oxidative stress due to the production of reactive oxygen species. In response to drought or salt stress, plants accumulate high concentrations of compatible osmolytes in the cytoplasm in order to adjust osmotic stress, in a process known as osmotic adjustment (Munns, 2002). These are small soluble molecules that are non-toxic at high concentrations in the cytoplasm, i.e., they do not affect cell metabolism. These molecules are crucial for cell turgor preservation by reducing the osmotic potential of the cell, increasing the cellular water retention. In addition, soluble osmolytes protect membranes and proteins from denaturing under stress conditions. Plants accumulate many molecules as osmolytes, including sucrose, fructose, glycerol, methylated inositols, trehalose, fructans, mannitol, sorbitol, Pro, and glycine betaine (Hasegawa et al., 2000). In this context, malate produced by PEPC could act as an osmolyte and/or provide carbon skeletons for compatible osmolyte synthesis (Doubnerová & Ryšlavá, 2011).

Although sorghum is a glycophyte, its salt exclusion strategy makes this crop relatively tolerant to salt stress (Chen et al., 2018) and it is ranked as a moderately salinity-tolerant crop (Mansour et al., 2021). Most studies on sorghum PEPC and its role in stress responses have been focused on the photosynthetic SbPPC1 isozyme. Salinity causes a moderate rise in PEPC activity in sorghum leaves, but a spectacular increase in PEPC phosphorylation and PPCK activity, both in light and darkness (Echevarría et al., 2001; García-Mauriño et al., 2003). This phenomenon is observed after at least 7 days of salt treatment by the ionic component of salt stress, in a process modulated by ABA (Monreal et al., 2007a,b). However, less is known about the participation of non-photosynthetic

PEPCs in stress responses in this important crop. Recently, it has been described that nitrogen stress in the form of excess ammonia induces Sb*PPC3* transcript abundance in sorghum roots and, to a lesser extent, in leaves (Arias-Baldrich et al., 2017). In addition, a rise in PEPC activity has been reported in C_3, C_4, and CAM plants in response to a variety of plant abiotic stresses such as drought, NaCl, or LiCl (Feria et al., 2016; González et al., 2003), cold (Crecelius et al., 2003), phosphate starvation (Chen et al., 2007; Feria et al., 2016; Gregory et al., 2009), cadmium or aluminum toxicity (Ermolayev et al., 2003; Willick et al., 2019), iron deficiency (López-Millán et al., 2000), or ozone stress (Dizengremel et al., 2009). In the C_3 plant *Arabidopsis thaliana*, salt stress increased PEPC activity, its phosphorylation state, and the content of L-malate in roots by increasing the expression of At*PPC3* (Feria et al., 2016). The PEPC family in *A. thaliana* is smaller than that in sorghum, with only four members (three PTPCs, AtPPC1–3, and one BTPC, AtPPC4) that are not closely related phylogenetically with sorghum PEPCs (Paterson et al., 2009).

Due to its abundance in sorghum seeds and in roots under ammonia stress, in the present work we studied the specific roles of the non-photosynthetic PEPC SbPPC3 by generating transgenic sorghum lines where the Sb*PPC3* gene was knocked down by RNA interference (RNAi) (*Ppc3* lines). *Ppc3* lines showed clear phenotypes, in both control and salt stress conditions, with affected stomatal opening, plant size, flowering, and productivity. Reduced Sb*PPC3* transcript abundance in *Ppc3* lines perturbed the plant metabolome, affecting the activity of metabolic enzymes accordingly, accumulating higher levels of stress indicators such as Asn, citrate, and sucrose in roots than wild-type (WT) plants, even in the absence of stress. We suggest SbPPC3, and orthologous non-photosynthetic PEPC proteins in other plants, as an important target to improve plant growth and productivity, in both control and stress conditions.

RESULTS

Knock-down of Sb*PPC3* decreases PEPC activity and protein levels in roots

To confirm the reduction in transcript abundance of the Sb*PPC3* gene, roots from hydroponically grown *Ppc3-1* and *Ppc3-2* lines were analyzed by quantitative PCR (qPCR), confirming a >90% decrease in Sb*PPC3* transcript abundance in plants expressing the RNAi construct compared to WT plants (Figure 1a). Moreover, Sb*PPC3* silencing induced a dramatic reduction on PEPC activity (Figure 1b) and immunoreactive PTPC polypeptides (Figure 1c) in roots from *Ppc3-1* and *Ppc3-2* compared to WT plants, supporting that this is the main PEPC isozyme in sorghum roots (Arias-Baldrich et al., 2017). The same parameters were analyzed in leaves. Because the photosynthetic SbPPC1 isozyme represents the vast majority of PPCs in leaves (Shenton et al., 2006), the reduction in Sb*PPC3* transcript abundance in this tissue (Figure 1d) was not translated into a decrease in total PEPC activity (Figure 1e) or immunoreactive PTPC polypeptides (Figure 1f) in leaves. In addition, the gene expression of Sb*PPC3* in roots from WT plants was found to be 32.2 ± 1.4 times higher than its expression in leaves (Figure 1a,d). Due to the similarities in nucleotide sequence among members of the Sb*PPC* family, we analyzed by qPCR whether unintended silencing of other members of the PEPC family occurred in *Ppc3* plants (Figure S1). Sb*PPC4–6* transcripts were not detected by qPCR in any tissue or condition analyzed, whereas Sb*PPC1* and Sb*PPC2* transcript abundance were not significantly affected in silenced plants.

Reduction of Sb*PPC3* transcript abundance affects plant growth and productivity

Non-photosynthetic PTPCs have many different important functions in plant physiology and metabolism (O'Leary et al., 2011), although the specific role and tissue-specific expression of different members of the PEPC family remain poorly understood. To study the specific role of SbPPC3 in plant growth and development, we grew WT, *Ppc3-1*, and *Ppc3-2* plants hydroponically, as described in the Experimental Procedures section, and analyzed several growth parameters. *Ppc3-1* and *Ppc3-2* plants showed a reduction in plant size after 4 weeks growing in hydroponic cultures compared to WT plants (Figure 2a). The reduction in size was accompanied by a slight decrease in biomass production in shoots (11 and 15% in *Ppc3-1* and *Ppc3-2*, respectively) (Figure 2b) and roots (12 and 5% in *Ppc3-1* and *Ppc3-2*, respectively) (Figure 2c). PEPC regulates stomatal opening by supplying malate as an osmolyte and counterion for K^+ influx in guard cells (Taiz et al., 2018). Interestingly, photosynthetic parameters analyzed showed a reduction in stomatal conductance (g_s) in *Ppc3-1* and *Ppc3-2* lines compared to WT plants (Figure 2d), although net photosynthesis (A) was only slightly affected in silenced lines (Figure 2e), likely due to the carbon concentration mechanism of C_4 plants. This effect on photosynthesis in silenced plants led to a rise in the intrinsic water use efficiency (iWUE), measured as the ratio of A to g_s (Bheemanahalli et al., 2021).

SbPPC3 is the main PEPC isozyme present during seed development (Ruiz-Ballesta et al., 2016). To analyze the effects of SbPPC3 on parameters related to seed production, WT, *Ppc3-1*, and *Ppc3-2* plants were grown in soil pots in the greenhouse until seeds were obtained, as described in the Experimental Procedures section. As in the case of hydroponic cultures, *Ppc3-1* and *Ppc3-2* plants showed a reduction in plant height (Figure 3a). *Ppc3-1* and *Ppc3-2* presented delayed flowering with respect to WT

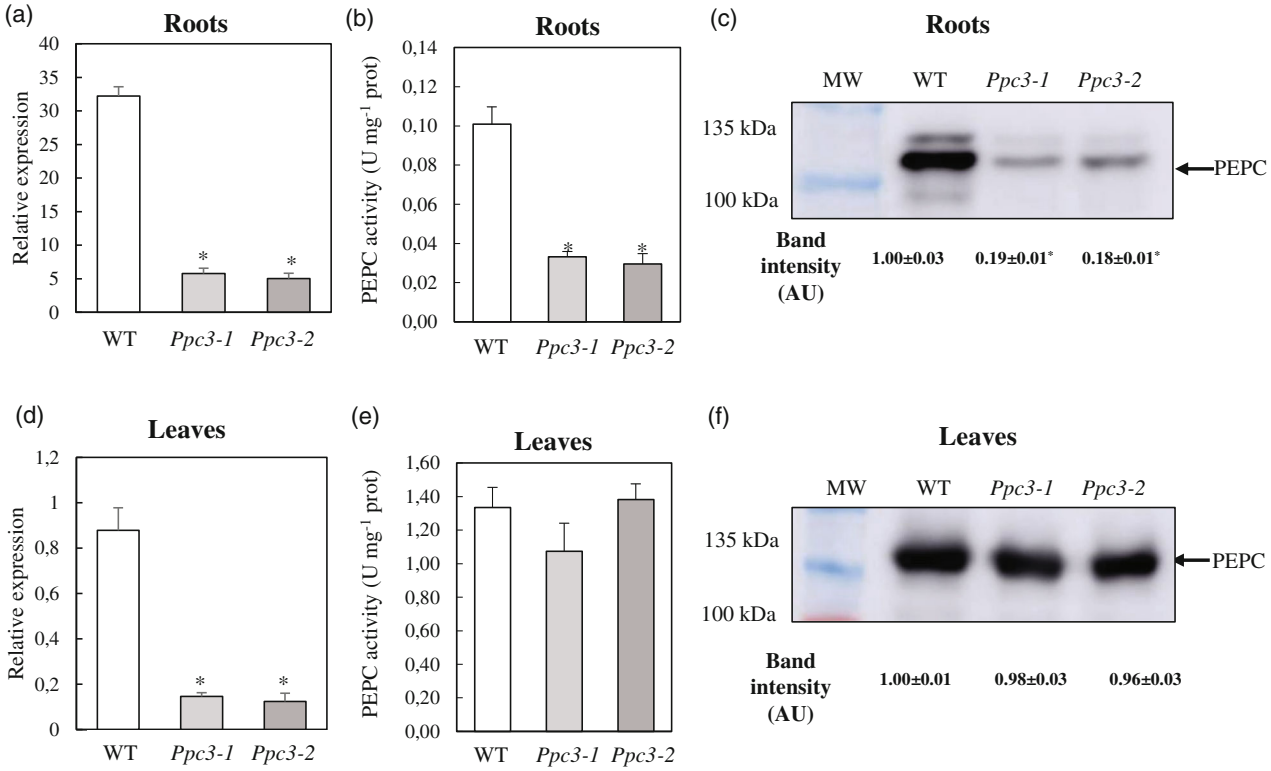

Figure 1. Effect of Sb*PPC3* silencing on PEPC activity and protein levels in roots and leaves. (a–c) Relative transcript abundance of Sb*PPC3* (a), PEPC activity (b), and immunodetection of PEPC (c) in roots from WT, *Ppc3-1*, and *Ppc3-2* plants. (d–f) Relative transcript abundance of Sb*PPC3* (d), PEPC activity (e), and immunodetection of PEPC (f) in leaves from WT, *Ppc3-1*, and *Ppc3-2* plants. In (a) and (d), transcript abundance is expressed relative to the transcript abundance in WT leaves. In (a), (b), (d), and (e), bars indicate mean ± SE (n = 3), where each biological sample is composed of three individual plants. *P < 0.05 vs. WT (t-test). In (c) and (f), 50 μg and 10 μg of total proteins per lane, respectively, was loaded for SDS-PAGE and transferred onto PVDF membranes for blotting using anti-PTPC antibodies, as described in the Experimental Procedures section. Signal intensity was measured using ImageStudio™ Lite software (LI-COR Biosciences). Values (mean ± SE, n = 4) are normalized to the WT value.

plants; at 60 days after germination, all WT plants presented panicles, whereas only 44 and 55% of *Ppc3-1* and *Ppc3-2* plants, respectively, had flowered (Figure 3b). At 90 days after germination, all plants had flowered. Sb*PPC3* silencing severely affected plant yield, with a marked reduction in the number of seeds produced per plant (Figure 3c). The reduction in seed production was not due to a change in the size of the panicle but due to a lower number of seeds per panicle in silenced lines compared to WT (Figure 3d). This effect on seed production could be of utmost importance for agriculture.

Sb*PPC3* expression is induced in response to salt stress only in roots

Most studies on salt stress in sorghum have analyzed the effects of salinity in leaves, focusing on photosynthetic SbPPC1. However, in other plants, the expression of non-photosynthetic PEPCs is induced in response to salt stress (Feria et al., 2016; González et al., 2003). In this work, we analyzed the impact of salt stress on WT and *Ppc3* plants to explore the significance of non-photosynthetic PEPC, both in leaves and roots. First, salinity moderately but significantly increased Sb*PPC3* transcript abundance in roots from WT plants (Figure 4a). This rise was accompanied by a consistent increase in PEPC activity (Figure 4b) and immunoreactive PTPC polypeptides (Figure 4c). However, in roots from *Ppc3-1* and *Ppc3-2*, the effect of salinity on Sb*PPC3* transcript abundance (Figure 4a), PEPC activity (Figure 4b), or immunoreactive PTPC polypeptides (Figure 4c) was totally abolished, indicating that SbPPC3 is the main PEPC protein participating in responses to salt stress in roots. In leaves, salinity had no impact on Sb*PPC3* transcript abundance, PEPC activity, or immunoreactive PTPC polypeptides in WT plants (Figure S2). As in control conditions, in stress conditions the silencing of Sb*PPC3* in leaves was not translated into a change in PEPC activity or quantity, most probably due to the dominating presence of SbPPC1.

Salt stress affects growth and photosynthetic parameters in sorghum plants

As expected, salt stress affected growth and photosynthetic parameters in all plants. NaCl treatment caused a

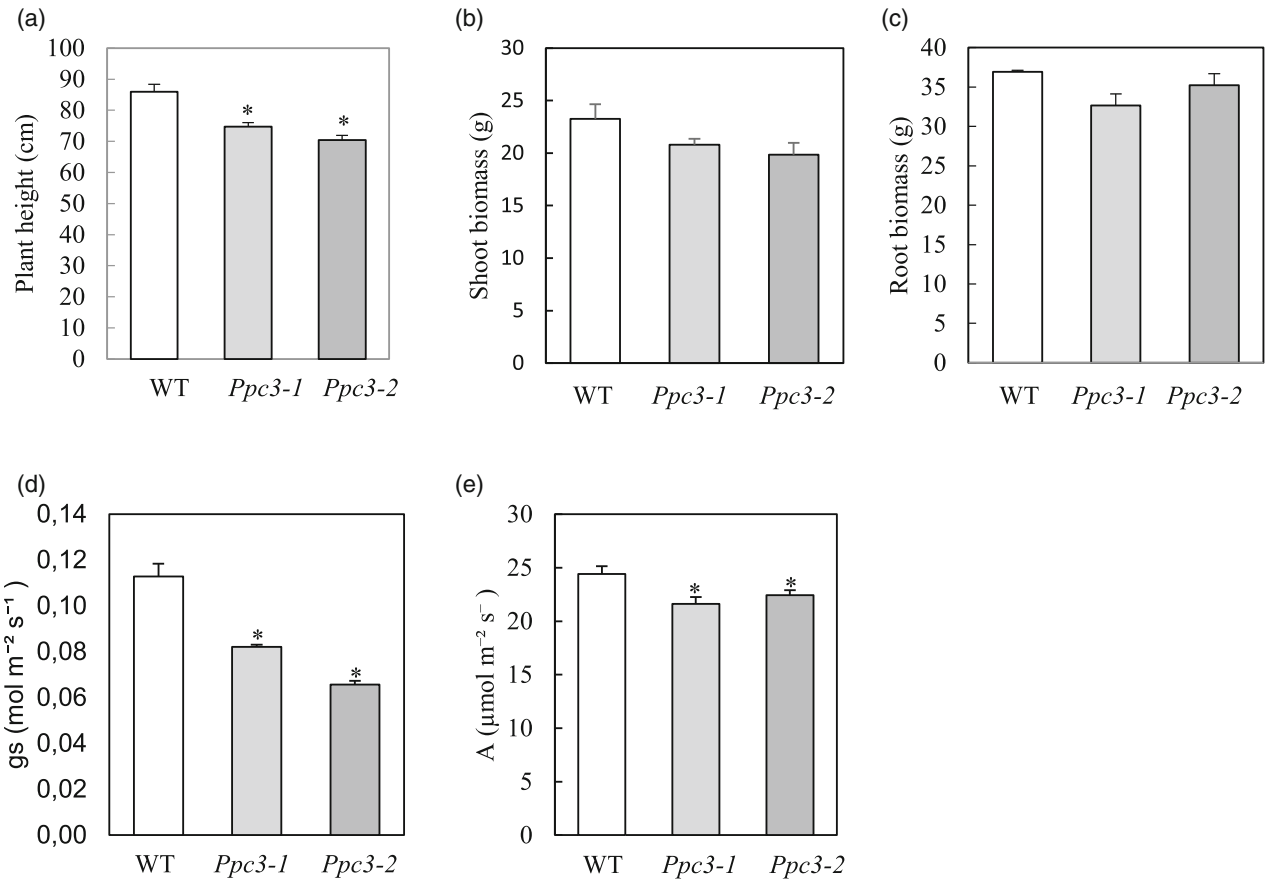

Figure 2. Effect of Sb*PPC3* silencing on growth and photosynthesis. (a–c) Plant height (a) and dry biomass from shoots (b) or roots (c) were analyzed in 4-week-old WT, *Ppc3-1*, and *Ppc3-2* plants grown hydroponically. (d,e) Stomatal conductance (g_s) (d) and net photosynthesis (A) (e) were measured in the youngest fully developed leaf at 350 µmol m^{-2} sec^{-1} PAR, a CO_2 concentration of 400 ppm, and ambient relative humidity, using a portable LI-6400XT photosynthesis analyzer (LI-COR). Bars indicate mean ± SE (n = 3), where each biological sample is composed of three individual plants. *P < 0.05 vs. WT (t-test).

marked reduction in plant height (Figure 5a) and biomass production in shoots (Figure 5b) and roots (Figure 5c), although no important differences were detected between WT and silenced plants, except for root biomass, which was further reduced in *Ppc3-1* plants. In addition, salt treatment affected photosynthesis in all plants by reducing g_s (Figure 5d) and A (Figure 5e). However, silenced plants showed lower g_s values compared to WT in response to salt, although the effect on A was dissimilar, with slightly higher values of A in silenced plants under salt stress. This apparent discrepancy might be due to the lower dependence of stomatal opening for CO_2 assimilation in C_4 plants.

To analyze the effects of salt stress on plant productivity, we carried out a greenhouse experiment watering plants with salty water (175 mM NaCl) as stated in the Experimental Procedures section. The reduction of plant size by salt stress was more pronounced in *Ppc3* plants compared to WT (Figure 6a,b). Interestingly, salinity affected flowering time in an opposite manner in WT plants or silenced plants, advancing flowering in the first and delaying this parameter in the second (Figure 6c). As in the case of control conditions, all salt-treated plants eventually flowered. Finally, salt stress markedly reduced productivity in all plants in terms of seed production, although this reduction was more dramatic in *Ppc3* plants (Figure 6d).

Silencing of Sb*PPC3* deeply disturbs central metabolism in control and salt stress conditions

Considering all important roles described for PEPC in plant central metabolism (O'Leary et al., 2011), we analyzed the effects of Sb*PPC3* silencing on sugar, amino acid, and organic acid contents in leaves and roots of *Ppc3-1* and WT plants grown hydroponically with or without salt by gas chromatography coupled to mass spectrometry (GC-MS), as described in the Experimental Procedures section.

To evaluate the overall differences in the metabolic profile of WT and *Ppc3-1* plants when exposed to salt, we constructed an unsupervised heatmap (Figure 7) and conducted principal component analysis (PCA) (Figure S3). The metabolites that were not detected in both organs, namely arabinose and lactate, were excluded from the

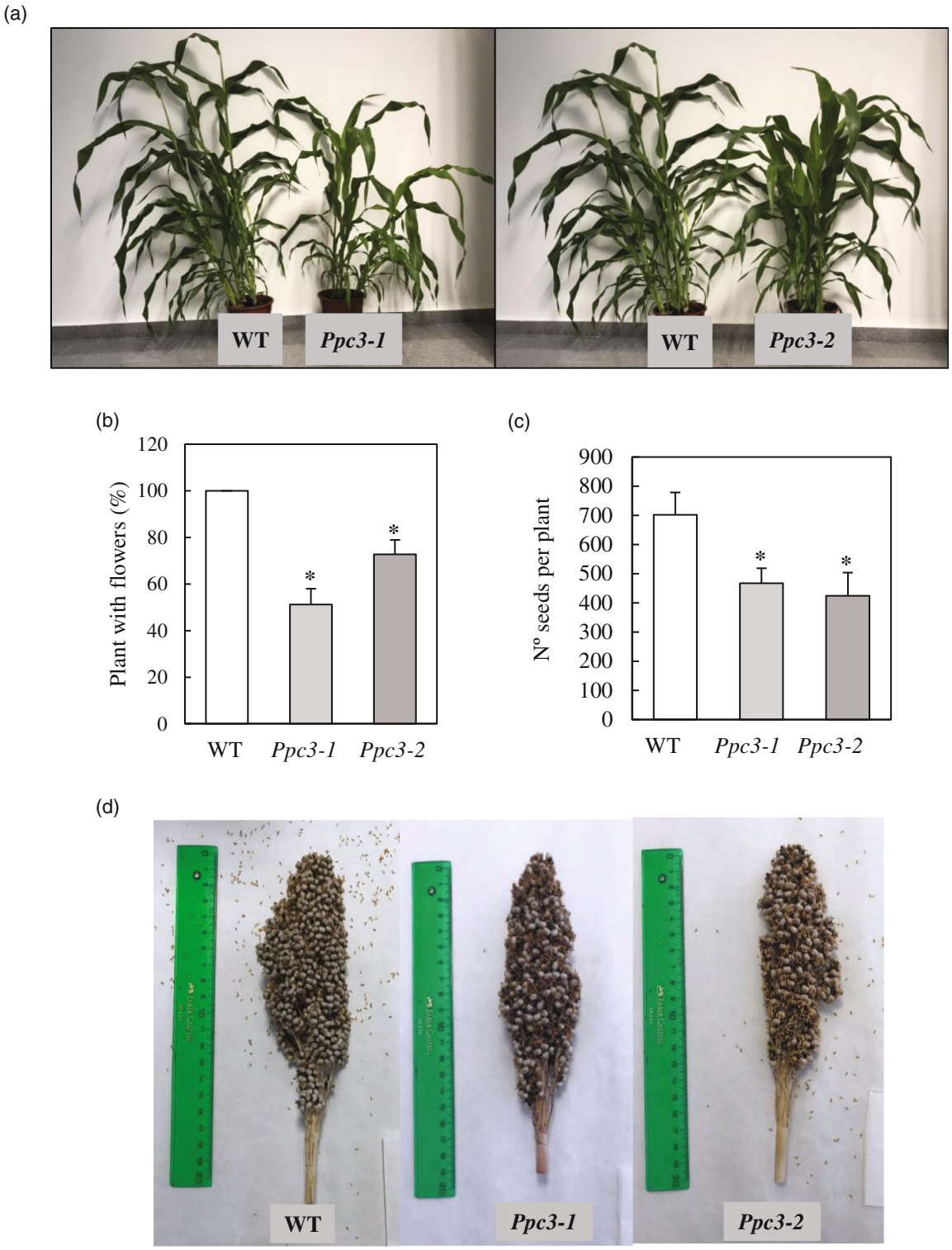

Figure 3. Effects of Sb*PPC3* silencing on plant productivity. Sorghum plants were grown in soil pots in the greenhouse for productivity experiments. (a) WT and *Ppc3-1* (left) and WT and *Ppc3-2* (right) sorghum plants 54 days after germination. (b) Percentage of flowered plants 60 days after germination. (c) Number of seeds per plant. For (b) and (c), bars indicate mean ± SE ($n = 3$), $^*P < 0.05$ vs. WT (*t*-test). (d) Representative image of sorghum panicles at the time of harvesting.

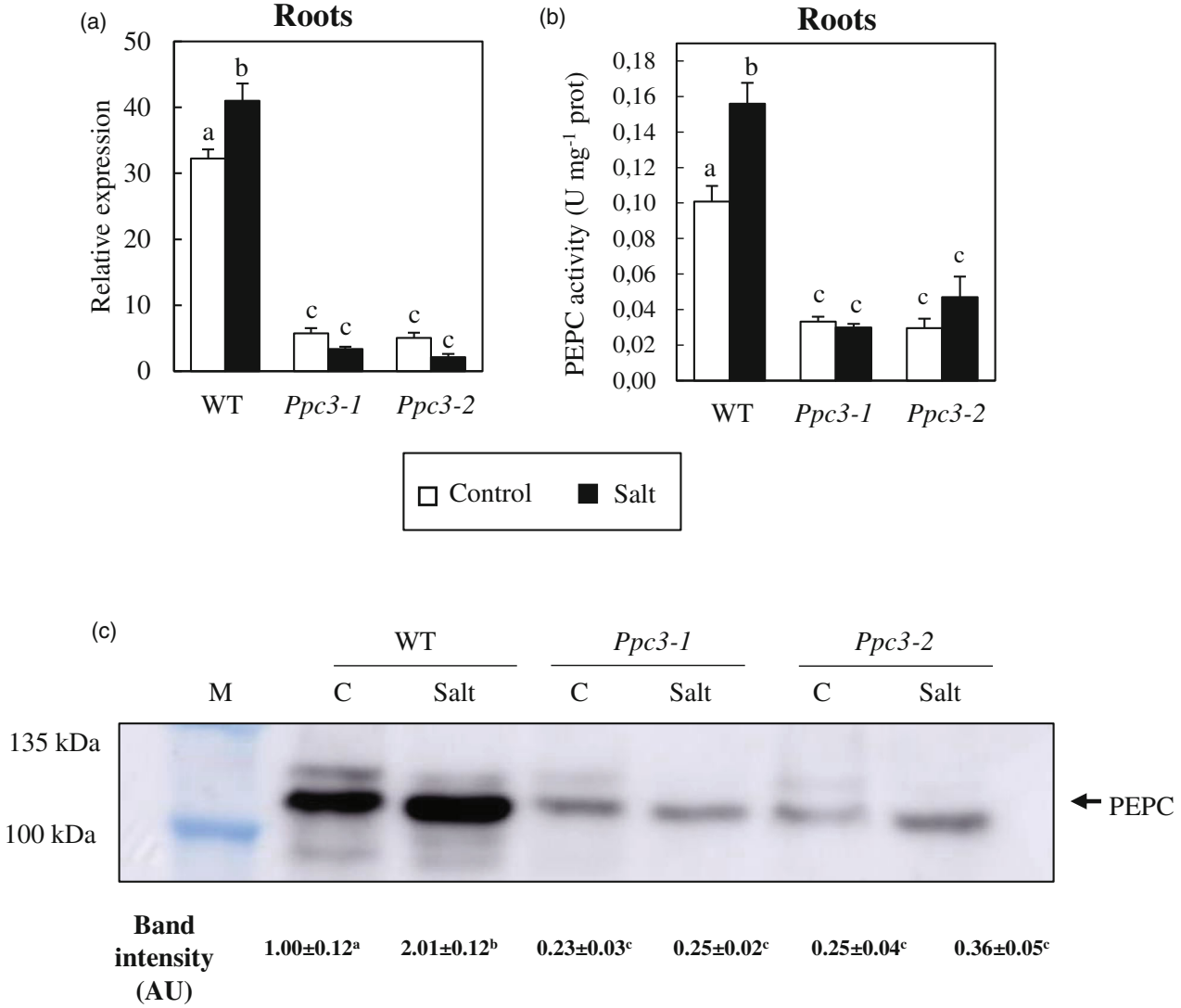

Figure 4. Effect of salinity on non-photosynthetic PEPC from sorghum roots. (a) Relative transcript abundance of Sb*PPC3* in sorghum roots from plants grown under control or salt stress conditions. Data are normalized to the transcript abundance of Sb*PPC3* in WT leaves in control conditions. (b) PEPC activity in sorghum roots. Bars indicate mean ± SE (n = 3), where each biological sample is composed of a pool of three individual plants growing in the same pot. Columns that do not have a common letter are significantly different by Duncan's multiple range test ($P < 0.05$). (c) Immunodetection of PEPC protein in sorghum root extracts from plants grown hydroponically under control (c) or salt stress (Salt) conditions. For analysis of protein levels, 50 μg per lane of total proteins was loaded for SDS-PAGE and transferred onto nitrocellulose membranes for blotting using anti-PTPC antibodies, as described in the Experimental Procedures section. Signal intensity was measured using ImageStudio™ Lite software (LI-COR Biosciences). Values (mean ± SE, n = 4) are normalized to the WT control (WT, C).

analysis. The first two principal components (PC1 and PC2) explained 76% of the total variance (Figure S3). The clustering shown in the heatmap clearly differentiated the organs with two main clusters being formed, corresponding to root and leaf. Besides, the effect of salt treatment was stronger than the effect of the mutation in both leaf and root. In general, salt treatment provoked more profound changes in the *Ppc3-1* background compared to the WT, notably at the root level (Figure 7).

In general, roots accumulated higher levels of amino acids than leaves in all plants (Table 1). In control conditions, silencing of Sb*PPC3* had opposite consequences on amino acid accumulation in leaves or roots, with a general drop in the former and a rise in the latter, except for Lys, whose level was reduced 4-fold in silenced roots compared to WT roots. Asn levels, on the contrary, were increased 4-fold in *Ppc3-1* roots compared to WT roots. On the other hand, salt stress raised the levels of free amino acids in leaves and roots, although in a different manner depending on the plant and the tissue. The biggest effect of salt stress in leaves was found in WT plants, whereas silenced plants showed a higher impact in roots, except for Asp and Lys, whose levels were half the levels found in WT roots. As expected, salinity induced a dramatic accumulation of

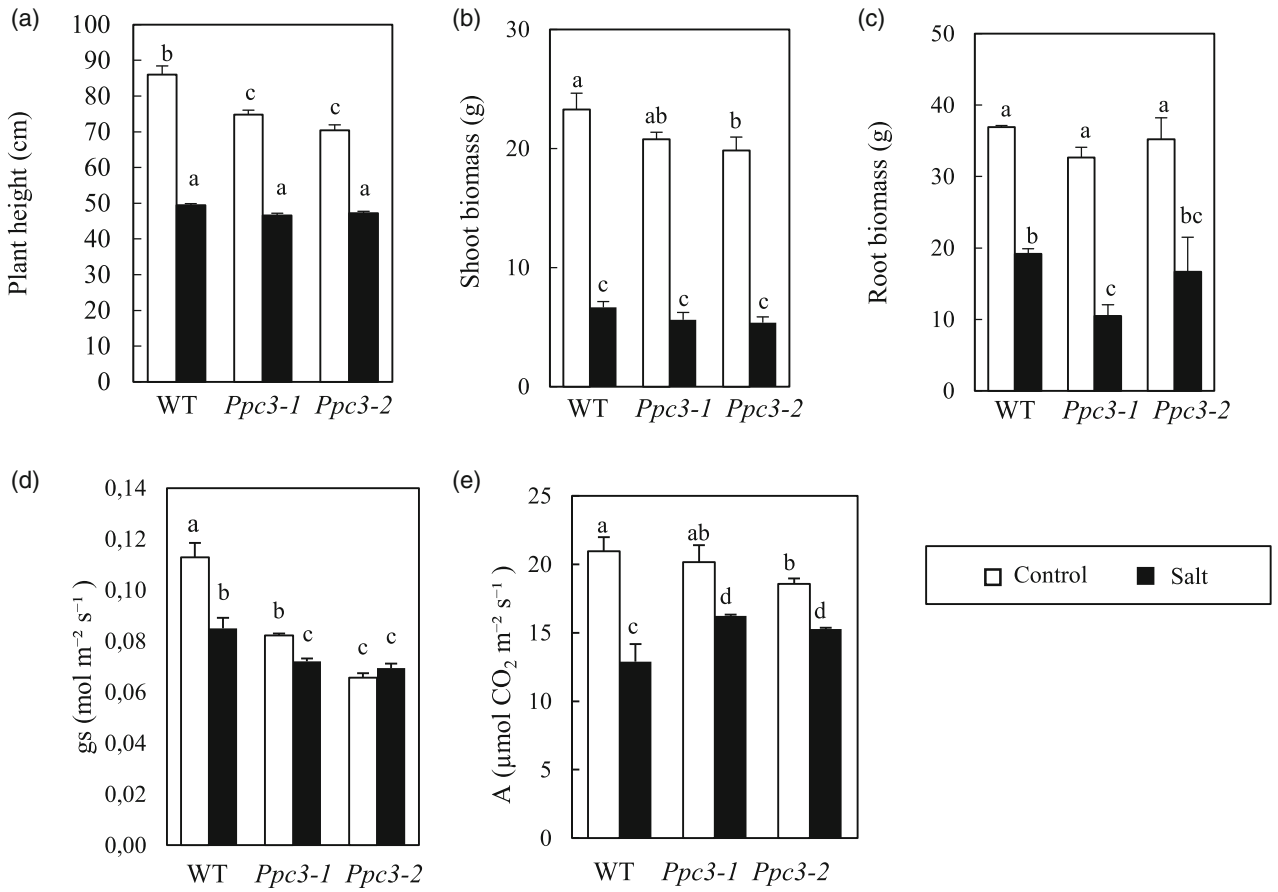

Figure 5. Effects of salinity on growth and photosynthesis in *Ppc3* plants. (a–c) Plant height (a) and dry biomass from shoots (b) and roots (c) were analyzed in 4-week-old WT, *Ppc3-1*, and *Ppc3-2* plants grown hydroponically under control or salt stress conditions, as indicated in the Experimental Procedures section. (d, e) Stomatal conductance (g_s) (d) and net photosynthesis (A) (e) were measured in the youngest fully developed leaf of hydroponically grown plants at 350 µmol m^{-2} sec^{-1} PAR, a CO_2 concentration of 400 ppm, and ambient relative humidity, using a portable LI-6400XT photosynthesis analyzer (LI-COR). Bars indicate mean ± SE (n = 3). Columns that do not have a common letter are significantly different by Duncan's multiple range test (P < 0.05).

Pro in leaves and roots of both plants, although higher values were found in leaves for WT and in roots for *Ppc3-1* plants. Amides Gln and Asn accumulated in roots of both WT and *Ppc3-1* plants under salt stress, although the levels found in silenced plants were 2-fold higher than those in WT plants. Notably, the highest impact on the accumulation of an amino acid was for Asn, with nearly 570-fold and 255-fold increases in roots of *Ppc3-1* and WT plants, respectively, compared to the levels in WT leaves in control conditions.

The TCA cycle organic acid anions succinate, malate, and citrate were more abundant in roots than in leaves in both lines, whereas the contrary was found for pyruvate and 2-oxoglutarate (2-OG) (Table 2). In leaves, *Ppc3-1* plants showed a slight reduction in the content of organic acid anions compared to WT plants in control conditions. In roots, the levels of malate, citrate, and 2-OG were higher in silenced plants than in WT, whereas no effect was found for succinate or pyruvate. Lactate levels were increased 3-fold in *Ppc3-1* roots compared to WT roots, indicating an activation of fermentation routes in silenced plants. Salinity had opposite effects on the accumulation of organic acid anions in leaves and roots, with a drop in leaves and a rise in roots. Citrate accumulated in higher amounts in roots in response to salt compared to the amounts detected in leaves from WT plants in control conditions. Compared with their respective controls, citrate levels were increased 3-fold and 2-fold by salt stress in WT roots and *Ppc3-1* roots, respectively. However, no effect of salinity on citrate levels was detected in leaves from any plant. Succinate levels were increased in silenced but not in WT roots and reduced in leaves of all plants. Malate levels were reduced in leaves and roots of silenced plants, but not affected in WT. Finally, pyruvate and 2-OG levels were reduced by salt stress in leaves of both lines, although the total amount was smaller for silenced leaves compared to WT. In roots, the effect of salt stress on these two organic acid anions was the opposite, with a rise in both plants but reaching higher amounts in silenced plants.

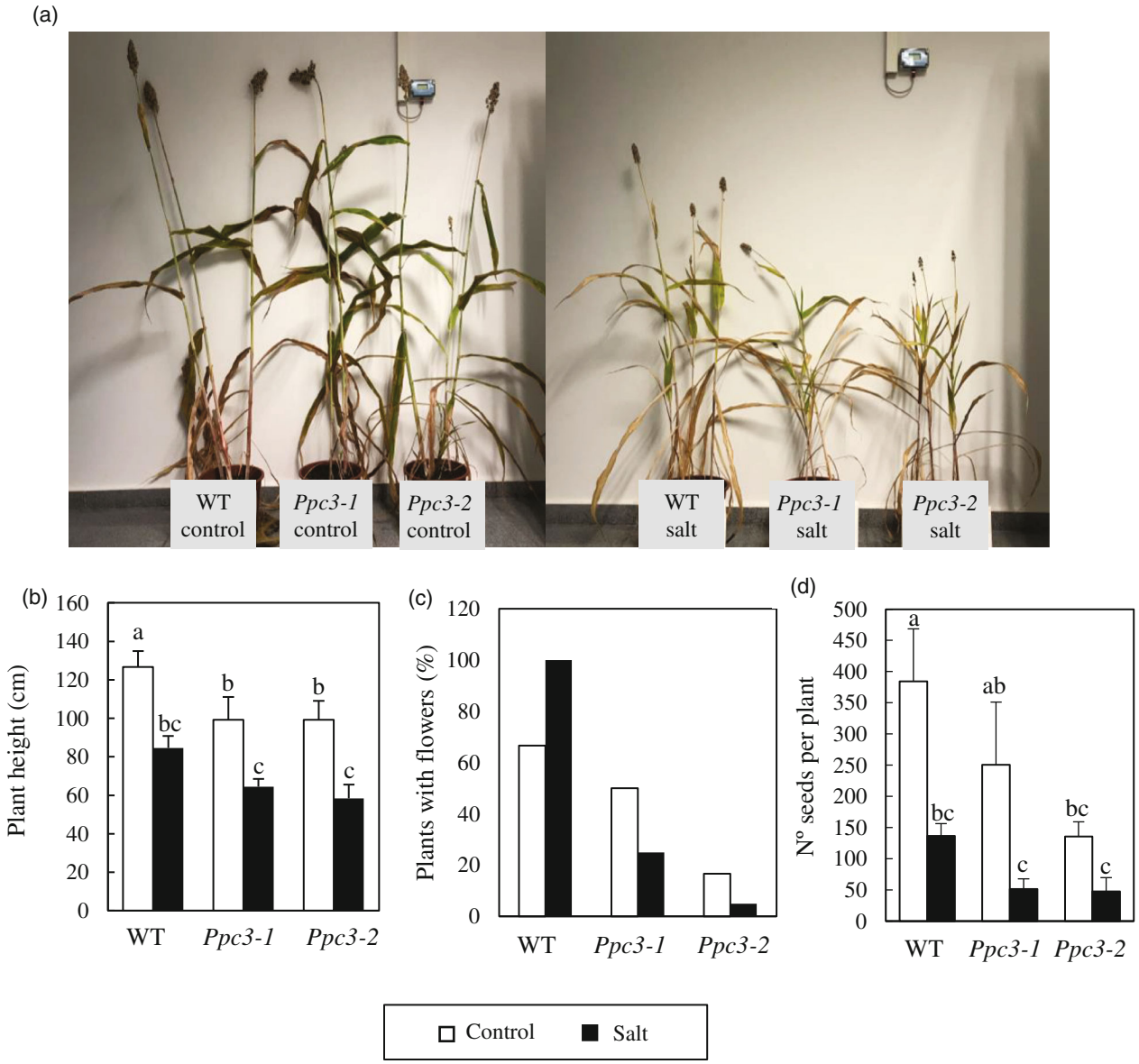

Figure 6. Effects of salt stress on plant productivity. Sorghum plants were grown in soil pots in the greenhouse and watered with water or salty water (175 mM NaCl), as indicated in the Experimental Procedures section. (a,b) Representative image of plants grown in control (left) or salt stress (right) conditions (a) and plant height (b) at the time of harvesting 6 months after germination. (c) Percentage of flowered plants 64 days after germination. (d) Number of seeds per plant. Bars indicate mean ± SE (n = 9), where each biological sample is composed of one individual plant. Columns that do not have a common letter are significantly different by Duncan's multiple range test ($P < 0.05$).

Finally, the sugar levels in leaves from *Ppc3-1* and WT plants were similar in control conditions (Table 3). However, in roots from silenced plants, we found a 4-fold increase in the content of sucrose compared to WT roots. Finally, glucose and fructose levels were not affected by Sb*PPC3* silencing in leaves or roots in control conditions. In response to salt stress, WT and *Ppc3-1* plants accumulated sucrose in leaves and roots and arabinose in roots, although the detected levels of both sugars in silenced plants were 2-fold higher than those in WT plants. The glucose and fructose levels in leaves dropped in silenced plants but not in the WT in response to salt stress, and no significant difference was found in roots.

To further study the impact of Sb*PPC3* silencing and/or salt stress on central metabolism, we analyzed the activity of enzymes implicated in C/N metabolism in leaves and roots of WT, *Ppc3-1*, and *Ppc3-2* plants, both in control and salt stress conditions. Citrate synthase (CS) activity was low in leaves for any plant or condition compared to roots (Figure 8a,b) and unaffected in any plant or upon any treatment, as was the level of citrate (Table 2). On the other hand, CS activity in roots was induced by salt stress in all

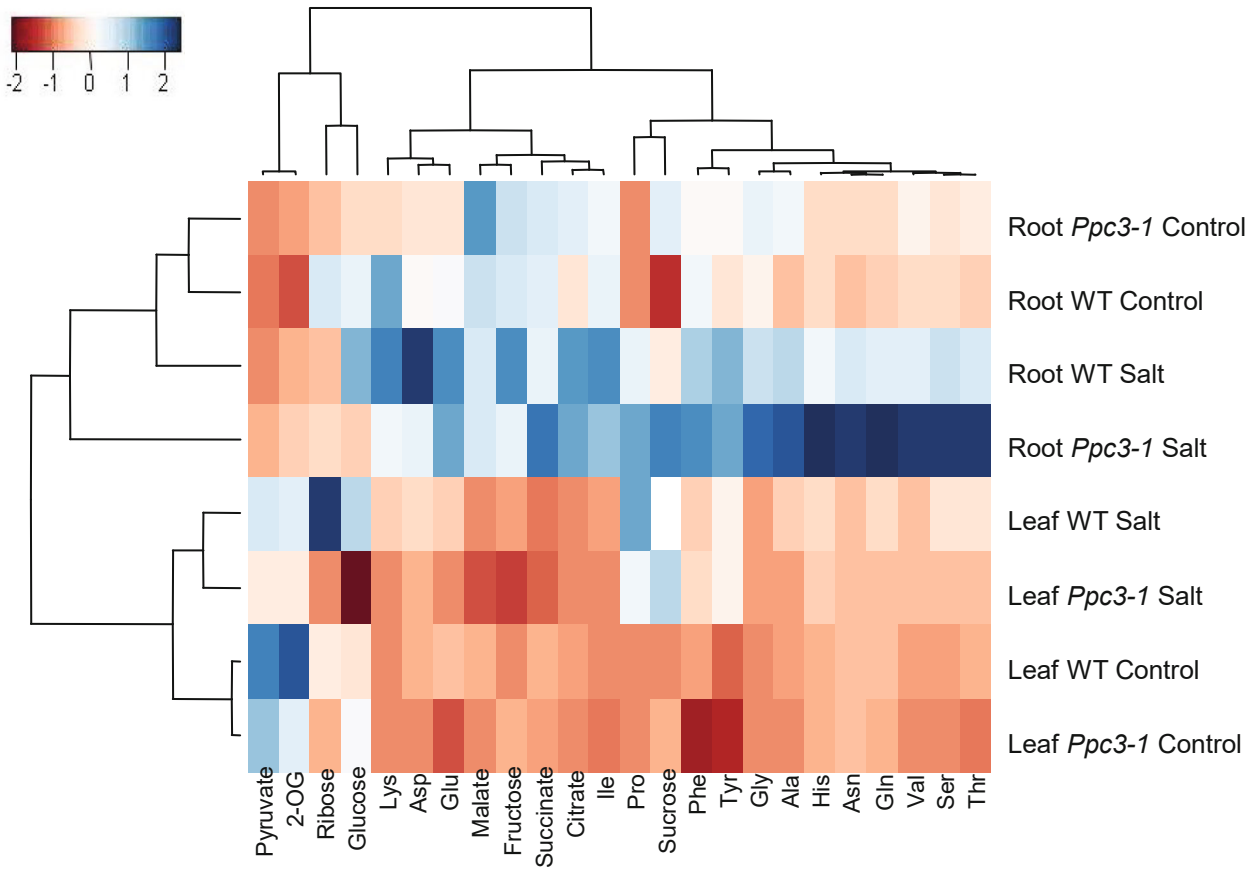

Figure 7. Heatmap analysis of detected primary metabolites. Heatmap representation of 24 metabolites determined in sorghum leaves and roots of WT or *Ppc3-1* plants under control or salt stress conditions (n = 3, each replicate corresponding to a pool of three individual plants).

plants, although the activity was higher in silenced plants than in WT plants, both in control and in salt stress conditions (Figure 8b). However, a more complex relationship was observed for other enzymes involved in the TCA cycle and organic acid anion metabolism. In roots, salinity slightly induced isocitrate dehydrogenase (ICDH) and pyruvate kinase (PK) activities in all lines (Figure S4). In leaves, no effect on ICDH of salt or silencing was found. PK activity in leaves was 10 times higher than in roots, concurring with the higher levels of pyruvate found in this tissue compared to roots (Table 2). Malic dehydrogenase (MDH), NAD-malic enzyme (NAD-ME), and NADP-malic enzyme

Table 1 Free amino acid contents in leaves and roots of WT and *Ppc3-1* plants treated with or without NaCl

Tissue	Line	Treatment	Ala	Ile	Val	Gly	Ser	Thr
Leaves	WT	Control	1 ± 0.06 a	1 ± 0.11 ab	1 ± 0.05 a	1 ± 0.04 a	1 ± 0.07 a	1 ± 0.07 a
		Salt	1.7 ± 0.11 b	1.4 ± 0.07 b	2.2 ± 0.29 ab	2 ± 0.48 a	3.4 ± 0.36 b	2 ± 0.16 b
	Ppc3-1	Control	0.5 ± 0.04 c	0.8 ± 0.08 a	0.6 ± 0.05 c	0.3 ± 0.04 b	0.3 ± 0.04 c	0.5 ± 0.04 c
		Salt	0.9 ± 0.06 a	1.10.08 ab	1.1 ± 0.04 a	1.1 ± 0.17 a	2 ± 0.23 d	1.3 ± 0.16 a
Roots	WT	Control	1.5 ± 0.23 ab	5.6 ± 1.21 c	3.4 ± 0.57 bd	11.3 ± 1.81 c	2.8 ± 0.47 bd	1.4 ± 0.24 a
		Salt	5.3 ± 0.41 d	9.4 ± 1.42 d	7.6 ± 0.94 e	20.8 ± 3.62 d	8.5 ± 0.74 e	3.7 ± 0.34 d
	Ppc3-1	Control	3.8 ± 0.41 e	5.2 ± 0.36 c	4.9 ± 0.35 d	16.1 ± 0.87 cd	3.3 ± 0.28 b	2.2 ± 0.16 b
		Salt	7.9 ± 0.51 f	7.8 ± 0.39 d	12.7 ± 0.7 f	33.6 ± 4.09 e	15.9 ± 1.81 f	6.9 ± 0.83 e

Samples from leaves or roots of hydroponically grown sorghum plants (WT and *Ppc3-1* lines) were analyzed by GC-MS as described in the Experimental Procedures section. The amount of each amino acid is expressed as arbitrary units relative to the value of that amino acid detected in leaves of WT plants in control conditions. Data are the mean of three independent experiments (n = 3). Means within a column that do not have a common letter are significantly different by Duncan's multiple range test (P < 0.05).

(NADP-ME) levels were reduced in leaves in response to salt stress but not affected in roots, although the effect was similar within the different sorghum lines (Figure S4).

On the other hand, nitrate reductase (NR) activity was higher in leaves (Figure 8c) than in roots (Figure 8d). No effect of salt or silencing was found in leaves, whereas in roots, salt stress induced NR activity only in silenced plants. NADH-glutamate synthase (GOGAT) was not detected in leaves (not shown) but its activity was induced in roots in response to salt, with silenced plants showing slightly higher activities than WT plants (Figure 8e). Glutamine synthetase (GS) was induced by salt stress in roots in all plants, whereas glutamate dehydrogenase (GDH) was not affected by salt or silencing in roots. In leaves, GS and GDH levels were slightly reduced by salt treatment in all plants. AAT levels were similar in all tissues and conditions analyzed (Figure S5).

DISCUSSION

In the present work, we studied the physiological roles of the non-photosynthetic PEPC isozyme SbPPC3 in sorghum plants by knocking down this gene by RNAi. Sb*PPC3* silencing was achieved in both leaves and roots in *Ppc3-1* and *Ppc3-2* lines, causing a reduction in PEPC activity and immunoreactive polypeptide levels in roots. However, no effect on total PEPC activity or protein was detected in leaves, likely due to the presence of the photosynthetic SbPPC1 protein (Shenton et al., 2006) and the small amounts of SbPPC3 found in leaves compared to roots (expression about 30 times higher in the latter according to current and previous results; Arias-Baldrich et al., 2017; Lepiniec et al., 2003). Nevertheless, Sb*PPC3* silencing had an important effect in leaves by reducing g_s. This finding is intriguing considering that SbPPC3 is considered a root/seed dominant PEPC isoform (Arias-Baldrich et al., 2017; Ruiz-Ballesta et al., 2016). In a microarray experiment in *A. thaliana* guard cells, At*PPC2* seemed to be the main PEPC isoform detected, being among the 50 most expressed genes in *A. thaliana* guard cells (Bates et al., 2012), indicating the importance of specific PEPC isoforms in the control of stomata. The AtPPC2 protein shares 85.14 and 84.05% sequence identity with SbPPC2 and SbPPC3, respectively. The effect on g_s found in *Ppc3* plants suggests that SbPPC3 may be the PEPC isozyme synthesizing malate as osmolyte for maximal stomatal opening (Outlaw, 1990; Taiz et al., 2018). However, we cannot totally rule out that this effect might be a consequence of root malfunctioning in silenced plants due to the predominant presence of SbPPC3 in this tissue. On the other hand, net photosynthesis was only slightly reduced in *Ppc3* plants, likely due to the lower dependency of C_4 plants on stomatal opening for CO_2 fixation (Sage et al., 2012). In addition, silencing of Sb*PPC3* reduced plant size and productivity, with fewer seeds produced per plant and delayed flowering, indicating a big impact of silencing on plant growth and reproduction. A reduction in plant size and a delay in flowering in *A. thaliana* PEPC knock-out mutants (Feria et al., 2016; Shi et al., 2015; Willick et al., 2019) and the abundance of SbPPC3 during seed development in sorghum have previously been described (Ruiz-Ballesta et al., 2016). In the present work, we found that the absence of SbPPC3 negatively impacts maximal stomatal opening, growth, and productivity.

PEPC is a ubiquitous enzyme playing key roles in plant central metabolism (O'Leary et al., 2011). Therefore, as expected, Sb*PPC3* silencing had important effects on the accumulation of sugars, amino acids, and organic acid anions, both in leaves and in roots, although again not in the same direction in both tissues. Silencing of Sb*PPC3* reduced the content of organic acid anions and amino acids in sorghum leaves but had little impact on sugars in control conditions. These results are in agreement with the classical view of non-photosynthetic PEPCs replenishing TCA intermediates withdrawn to support anabolism and N assimilation (O'Leary et al., 2011). Thus, lower amounts of SbPPC3 in leaves would be translated into a decrease in

Phe	Asp	Asn	Glu	Gln	His	Lys	Tyr	Pro
1 ± 0.06 ab	1 ± 0.04 a	1 ± 0.15 a	1 ± 0.1 a	1 ± 0.07 a	1 ± 0.03 a	1 ± 0.08 a	1 ± 0.03 a	1.2 ± 0.12 a
1.2 ± 0.10 bc	2.3 ± 0.3 b	2.1 ± 0.25 b	1.1 ± 0.0 a	3.7 ± 0.38 abd	3.1 ± 0.46 b	4.6 ± 0.64 b	1.9 ± 0.20 b	62.9 ± 11.3 b
0.4 ± 0.03 a	0.4 ± 0.1 c	0.7 ± 0.13 a	0.4 ± 0.0 b	0.3 ± 0.03 b	1 ± 0.18 a	0.7 ± 0.06 a	0.7 ± 0.06 a	1.2 ± 0.2 a
1.3 ± 0.37 bc	1.1 ± 0.1 a	0.5 ± 0.09 a	0.7 ± 0.0 c	2.1 ± 0.58 abd	2.3 ± 0.04 ab	1.4 ± 0.23 a	1.9 ± 0.46 b	44.5 ± 6.0 c
1.7 ± 0.30 cd	3.7 ± 1.0 b	10.9 ± 1.62 c	1.6 ± 0.2 d	2.3 ± 0.30 a	3.2 ± 0.86 ab	19.4 ± 5.59 c	1.7 ± 0.30 b	4.6 ± 1.8 a
2.2 ± 0.28 de	10.9 ± 2.2 d	254.9 ± 39.95 d	2.7 ± 0.1 e	15.5 ± 2.41 c	8.5 ± 1.18 c	22.3 ± 5.51 c	2.8 ± 0.30 c	49.9 ± 4.3 bc
1.6 ± 0.18 cd	2.5 ± 0.2 b	47.2 ± 10.18 e	1.2 ± 0.1 ad	3.9 ± 0.34 d	3.0 ± 0.30 b	5.8 ± 0.45 b	2 ± 0.14 b	1.9 ± 0.3 a
2.5 ± 0.06 e	4.8 ± 0.3 e	566.9 ± 92.91 f	2.5 ± 0.2 e	38.7 ± 5.22 e	20.9 ± 2.66 d	10.8 ± 0.59 d	2.9 ± 0.12 c	80 ± 8.0 d

Table 2 Organic acid anions content in leaves and roots of WT and *Ppc3-1* plants treated with or without NaCl

Tissue	Line	Treatment	Citrate (AU)	Lactate (AU)	Malate (AU)	Pyruvate (AU)	Succinate (AU)	2-OG (AU)
Leaves	WT	Control	1 ± 0.06 a	n.d.	1 ± 0.08 a	1 ± 0.09 a	1 ± 0.13 a	1 ± 0.07 a
		Salt	0.78 ± 0.06 a	n.d.	0.72 ± 0.04 a	0.64 ± 0.10 b	0.46 ± 0.02 b	0.61 ± 0.06 b
	Ppc3-1	Control	0.81 ± 0.05 a	n.d.	0.69 ± 0.05 a	0.8 ± 0.08 b	0.72 ± 0.03 a	0.62 ± 0.06 b
		Salt	0.83 ± 0.16 a	n.d.	0.23 ± 0.01 b	0.37 ± 0.02 c	0.39 ± 0.02 b	0.43 ± 0.03 c
Roots	WT	Control	7.22 ± 0.64 b	1 ± 0.13 a	2.72 ± 0.11 c	0.04 ± 0.01 d	2.66 ± 0.17 c	0.12 ± 0.01 e
		Salt	23.87 ± 1.68 c	1.81 ± 0.15 b	2.57 ± 0.20 c	0.09 ± 0.02 d	2.46 ± 0.46 c	0.26 ± 0.03 d
	Ppc3-1	Control	14.49 ± 0.99 d	3.12 ± 0.26 c	3.61 ± 0.16 d	0.1 ± 0.01 d	2.88 ± 0.11 c	0.25 ± 0.03 d
		Salt	23.2 ± 1.00 c	3.49 ± 0.26 c	2.63 ± 0.29 c	0.17 ± 0.02 d	4.3 ± 0.57 d	0.34 ± 0.04 cd

Samples from leaves or roots of hydroponically grown sorghum plants (WT and *Ppc3-1* lines) were analyzed by GC-MS as described in the Experimental Procedures section. The amount of each organic acid is expressed as arbitrary units relative to the value of that organic acid detected in leaves of WT plants in control conditions. Data are the mean of three independent experiments ($n = 3$). n.d., not detected; 2-OG, 2-oxoglutarate. Means within a column that do not have a common letter are significantly different by Duncan's multiple range test ($P < 0.05$).

Table 3 Sugar content in leaves and roots of WT and *Ppc3-1* plants treated with or without NaCl

Tissue	Line	Treatment	Arabinose (AU)	Fructose (AU)	Glucose (AU)	Ribose (AU)	Sucrose (AU)
Leaves	WT	Control	n.d.	1 ± 0.03 a	1 ± 0.02 a	1 ± 0.05 ab	1 ± 0.02 ab
		Salt	n.d.	1.16 ± 0.16 a	1.40 ± 0.10 a	2.03 ± 0.19 c	1.47 ± 0.10 c
	Ppc3-1	Control	n.d.	1.41 ± 0.2 a	1.18 ± 0.09 a	0.75 ± 0.08 a	1.19 ± 0.05 bc
		Salt	n.d.	0.35 ± 0.08 b	0.28 ± 0.03 b	0.65 ± 0.08 a	2.31 ± 0.09 d
Roots	WT	Control	0.74 ± 0.17 a	3.41 ± 0.53 c	1.27 ± 0.27 a	1.33 ± 0.25 b	0.63 ± 0.24 a
		Salt	1.57 ± 0.13 b	4.72 ± 0.99 c	1.57 ± 0.37 a	0.78 ± 0.05 a	1.59 ± 0.34 c
	Ppc3-1	Control	0.54 ± 0.03 a	3.65 ± 0.21 c	0.97 ± 0.06 a	0.76 ± 0.08 a	2.06 ± 0.08 cd
		Salt	3.32 ± 0.34 c	3.14 ± 0.08 c	0.90 ± 0.02 a	0.87 ± 0.06 ab	2.86 ± 0.02 e

Samples from leaves or roots of hydroponically grown sorghum plants (WT and *Ppc3-1* lines) were analyzed by GC-MS as described in the Experimental Procedures section. The amount of each sugar is expressed as arbitrary units related to the value of that sugar detected in leaves of WT plants in control conditions. Data are the mean of three independent experiments ($n = 3$). n.d., not detected. Means within a column that do not have a common letter are significantly different by Duncan's multiple range test ($P < 0.05$).

the accumulation of organic acid anions and amino acids due to its role in the control of C/N metabolism (Huppe & Turpin, 1994; Sweetlove et al., 2010). However, the similar levels of malate found in leaves from WT and silenced plants suggest that SbPPC3 may not be the main anaplerotic PEPC isozyme in this tissue. On the other side, the picture in roots was more complicated. Silencing of Sb*PPC3* raised the amounts of most amino acids, except for Lys, in particular Asn. Furthermore, the levels of organic acid anions, especially malate and citrate, were elevated and CS activity was increased. In addition, silenced roots accumulated sucrose and lactate, suggesting a possible activation of fermentation routes in this tissue due to a partial block of glycolysis (Taiz et al., 2018). The accumulation of organic acid anions like citrate (Che-Othman et al., 2017), malate (Doubnerová & Ryšlavá, 2011), or lactate (Taiz et al., 2018), together with a higher CS activity (Liang et al., 2021), and increases in the levels of amino acids like Asn (Rashmi et al., 2019), or sugars such as sucrose (Sánchez et al., 2008), are all responses that are triggered in many plants in response to stress, and *Ppc3* plants do so even in the absence of any stress. Moreover, the reduction in size or productivity found in silenced plants are typical consequences of stress (Lamers et al., 2020). Similar results have been shown in *A. thaliana*, where an At*PPC3* knock-out mutant showed a stressed phenotype in control conditions (Feria et al., 2016; Willick et al., 2019). The higher levels of malate found in roots from silenced compared to WT plants suggest that, as in the case of leaves, SbPPC3 may not be the main anaplerotic PEPC isozyme in this tissue.

Salt stress increases the abundance of Sb*PPC3* transcripts, PEPC activity, and immunoreactive PEPC polypeptide levels in sorghum roots but not in leaves. Several authors have described the induction of non-photosynthetic PEPCs in responses to salt stress, mainly in roots (Doubnerová & Ryšlavá, 2011; Feria et al., 2016; González et al., 2003; O'Leary et al., 2011). The effect of salinity on SbPPC3 in roots was observed after days of treatment, suggesting that, as for SbPPC1 and SbPPCK1 in leaves (García-Mauriño et al., 2003), the ionic component of salt stress may the factor triggering the induction of PEPC in sorghum roots (Munns, 2002).

It is widely known that salinity decreases photosynthetic parameters in plants (Munns & Tester, 2008; Shi

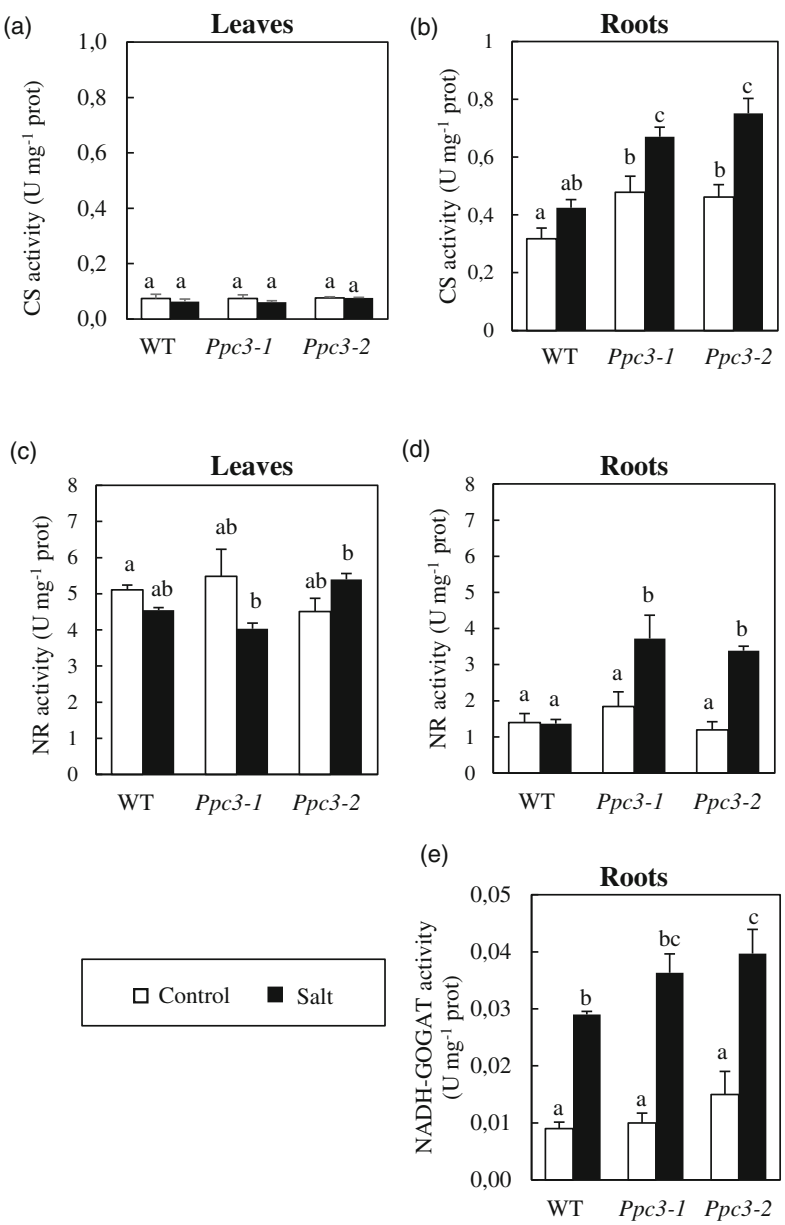

Figure 8. Effects of Sb*PPC3* silencing and salt stress on enzymatic activities related with C/N metabolism. Enzymatic activities were analyzed spectrophotometrically in leaves and roots from hydroponically grown sorghum plants, as described in the Experimental Procedures section. (a–e) Citrate synthase (CS) in leaves (a) and roots (b), nitrate reductase (NR) in leaves (c) and roots (d), and NADH-glutamate synthase (GOGAT) in roots (e). Bars indicate mean ± SE ($n = 3$), where each biological sample is composed of three individual plants. Columns that do not have a common letter are significantly different by Duncan's multiple range test ($P < 0.05$).

et al., 2015). As expected, salt stress severely reduced g_s and A in all plants. However, silenced plants showed lower levels of g_s, whereas the opposite was found for A, with WT plants showing lower rates of C fixation than *Ppc3* plants under salt stress. Although a clear difference between WT and silenced *Ppc3* plants was not found in young plants, when extending the salt treatment to the whole life cycle of the plants, *Ppc3* plants were found to be more sensitive to stress than WT plants, as reflected by the higher impact of salt on size, flowering, and productivity in *Ppc3-1* and *Ppc3-2* plants compared to WT.

A change in the balance between central metabolites, such as amino acids and organic acid anions, constitutes a conserved metabolic response of plants to salt stress (Sánchez et al., 2008). Our results showed accumulation of amino acids, mainly Pro, and a drop in organic acid anions in leaves. However, the levels of these primary metabolites were lower in silenced plants compared to WT, as already found in control conditions (O'Leary et al., 2011). In addition, *Ppc3-1* plants experienced a rise in sucrose levels and a drop in glucose and fructose contents in leaves in response to salt, whereas WT plants did not. The accumulation of sucrose and amino acids, and the decrease in organic acid anions, seems to be a conserved response to salt stress (Sánchez et al., 2008).

In roots, silenced plants accumulated higher levels of sucrose in any condition, suggesting that a partial block of glycolysis was happening in this tissue (Bandehagh & Taylor, 2020). This partial block of carbohydrate catabolism in roots from silenced plants was further evidenced by the accumulation of lactate in this tissue. The accumulation of sucrose in silenced plants could itself be a driving factor for phenotypic differences found in these plants. As in the case of leaves, both WT and *Ppc3-1* plants raised the levels of amino acids in response to salt stress, but in this case, all amino acids, except for Lys and Asp, were found in equal or higher amounts in silenced plants compared to WT, particularly Pro, Asn, or Gln. In addition, NR was activated by salt only in silenced plants, and GOGAT was activated in all plants but at higher levels in *Ppc3* compared to WT roots. Altogether, these results suggest that silencing of Sb*PPC3* in roots induces a shift toward the synthesis of molecules with a higher N/C ratio due to a limitation in C metabolism (Herrera-Rodríguez et al., 2007; Lea, 1997; Mansour, 2000). The accumulation of Asn and Gln, together with Pro or sucrose, is a general response to salt stress and the higher levels found in *Ppc3* plants may indicate a higher degree of stress in these plants (Ma et al., 2018; Rashmi et al., 2019; Ushakova et al., 2006; van Zelm et al., 2020).

In contrast to leaves, levels of pyruvate, 2-OG, and, more importantly, citrate were higher in roots in response to salt stress in all plants. However, *Ppc3-1* plants, but not WT, accumulated succinate and reduced malate content in roots in response to salt, indicating an effect of Sb*PPC3* silencing on the TCA cycle (O'Leary et al., 2011). Malate synthesized via PEPC and NAD-MDH could act as a vacuolar osmolyte and as a transport metabolite to export reducing equivalents out of the chloroplast (Crecelius et al., 2003). However, in the present study, malate did not accumulate in any tissue or any plant in response to salt stress, but citrate did, together with CS activity, indicating that sorghum could perhaps use citrate instead of malate as an osmolyte. Interestingly, overexpression of a CS isozyme improved salt tolerance in maize (*Zea mays*) plants (Liang et al., 2021).

Although some of our results may at first be surprising, e.g., a more dramatic drop in malate content in roots from silenced plants could have been hypothesized, the effects of SbPPC3 silencing on plant performance, in both control and stress conditions, indicate the importance of SbPPC3 for plant metabolism and stress responses. The lack of correlation between malate levels and PEPC activity suggests that SbPPC3 may not be the main enzyme responsible for overall malate levels in control conditions at the whole plant level. This could be different in specific physiological contexts, for instance guard cells, developing seeds, or root apical cells. In addition, SbPPC3 has key roles in stresses that increase root PEPC activity, such as salinity or ammonium stress (Arias-Baldrich et al., 2017). For example, the salt-induced metabolic shift toward N-rich compounds (Asn, Gln) was more dramatic in *Ppc3* roots than in WT. Respiration in plant cells is characterized by the presence of alternative metabolic routes where C or electrons pass from one point to another by different enzymatic pathways (O'Leary et al., 2019). Moreover, many glycolytic enzymes, such as PEPC, can be regulated by PTMs, which further tunes its activity to the actual cellular conditions. This allows a level of complexity, diversity, and flexibility within plant glycolysis that may be important to surpass stressful situations, but makes it difficult to predict the results of a single enzyme modification within central metabolism. It is not unusual to find little impact in transgenic plants where a single glycolytic enzyme has been eliminated or silenced.

Apart from salt stress, non-photosynthetic PEPCs have been described to be activated or to participate in responses to other abiotic stresses affecting primarily roots, e.g., phosphate starvation (Chen et al., 2007; Gregory et al., 2009; Toyota et al., 2003), iron deficiency (Arias-Baldrich et al., 2015; López-Millán et al., 2000), cadmium or aluminum toxicity (Nocito et al., 2008; Wang et al., 2013; Willick et al., 2019), or nitrogen stress (Arias-Baldrich et al., 2017; Lasa et al., 2002). Hence, SbPPC3 may be important for root responses to these chemicals. SbPPC3 will be the objective of future works taking advantage of the *Ppc3* sorghum lines.

CONCLUSION

Taken together, our results show that although SbPPC3 is predominantly a root protein, its absence causes deep changes in plant physiology and metabolism in roots and leaves, negatively affecting maximal stomatal opening, growth, productivity, and stress responses in sorghum plants. The consequences of Sb*PPC3* silencing suggest that this protein, and maybe orthologs in other plants, could be an important target to improve plant growth, productivity, and resistance to salt stress and other stresses where non-photosynthetic PEPCs may be implicated.

EXPERIMENTAL PROCEDURES

Plant material and growth conditions

Sorghum (*S. bicolor* L.) WT and *Ppc3* plants used in this study correspond to the public genotype P898012. Seeds were surface sterilized with 50% (v/v) bleach and 0.1% Triton X-100 for 30 min and rinsed 8–10 times with sterile water. Seeds were placed in moist sterile filter papers for 3 days in darkness at 25°C. For hydroponic experiments, three seedlings were transferred to 1-L polyethylene pots filled with nitrate-type nutrient solution (Hewitt, 1966) and grown in 12/12 h light/dark cycles (25°C, 60% relative humidity and 20°C, 70% relative humidity, respectively), at a light intensity of 350 μmol m^{-2} sec^{-1} PAR light. Four weeks after germination, two to three fully expanded young leaves or total roots were

collected, ground with a mortar and pestle with liquid nitrogen, and stored at −80°C until use. Each biological replicate was composed of tissue from three individual plants growing within the same pot. For salinity experiments, plants grown hydroponically for 1 week were acclimated to salt by weekly increasing the NaCl concentration (86 and 175 mM final concentration) in the culture medium. Leaves and roots were harvested 1 week after applying the maximal NaCl concentration. For greenhouse experiments, seedlings were transferred to soil pots in the greenhouse (CITIUS, University of Sevilla, Sevilla, Spain) and watered three times a week with water for control experiments or two times with water and one time with salty water (175 mM NaCl) for salt stress experiments, until obtaining the seeds 6 months later. To block cross-fertilization between transformed plants, panicles were covered with paper bags. All samples were harvested within the first 3 h of the light period.

Vector construction and *Agrobacterium*-mediated transformation

The binary vector pFGC161 (Do et al., 2016), designed for gene silencing in cereals, was used to construct the hairpin RNA (hpRNA) cassettes. The T-DNA of the vector contained the selection gene *bar* under the control of the *Ubi1* intron promoter and the silencing cassette with two restriction sites separated by a rice (*Oryza sativa*) *waxy* intron driven by the CaMV 35S promoter (Gasparis et al., 2011). The hpRNA cassette constructed contained a specific 300-bp fragment of the Sb*PPC3* gene (bases 1260–1560 in the coding sequence; Figure S6) in the sense and anti-sense orientations. This fragment was amplified by PCR using the high-fidelity Q5 DNA polymerase (New England Biolabs, Ipswich, MA, USA) and cDNA from sorghum roots and purified by gel purification. The sequences of the primers used were: (forward) 5′-ATACTAGTGGCGCGCCATAGCTGACGGAAGTCTT-3′ and (reverse) 5′-CCGAGCTCGCCTAGGGCCAAAGCAATCTGCTGG-3′ (Table S1). The 300-bp fragment was inserted in sense and anti-sense orientations between *Asc*I and *Avr*II and between *Sac*I and *Spe*I restriction sites, respectively. The ligation product was used to transform *Escherichia coli* strain DH5α by heat shock, and single colonies were selected and grown on LB containing kanamycin as a selective marker. Correct cloning was confirmed by restriction analysis and sequencing. A schematic structure of the T-DNA of the vector pFGC161-PPC3 is presented in Figure S7.

Insertion of the vector pFGC161-PPC3 into *Agrobacterium tumefaciens* strain AGL1 and transformation of immature embryos from sorghum genotype P898012 were carried out at the Plant Transformation Core Facility, University of Missouri (USA) (https://plantsciencesweb.missouri.edu/plantbiotechlab/), following the method described by Do et al. (2018).

A total of 14 T0 plants (named A–N) from independent insertion events were obtained, and the T1 plants from all 14 T0 plants were analyzed in order to confirm the insertion of the T-DNA, classified depending on the degree of Sb*PPC3* silencing, and self-propagated to select homozygous T2 *Ppc3* lines.

Seeds from WT and *Ppc3* plants used in this study were sown, grown, and harvested in the same conditions and time, corresponding to the same batch.

Selection of transformed *Ppc3* plants

T1 plants harboring the T-DNA for Sb*PPC3* silencing were selected first by treatment with the herbicide ammonium glufosinate (Do et al., 2016) (Figure S8). Plants showing herbicide toxicity were discarded from further analysis. Second, PCR analysis was carried out on the *Ppc3* plants with no ammonium glufosinate symptoms, in order to detect the presence of *bar* and *waxy* genes in the genome, using 200 ng of genomic DNA, iTaq DNA polymerase (Intron Biotechnology, Burlington, MA, USA), and the specific primers (barF: 5′-AAACCCACGTCATGCCAGTT-3′, barR: 5′- CATCGAGA CAAGCACGGTCA-3′; waxyF: 5′-GTAGCCGAGTTGGTCAAAGGA-3′, waxyR: 5′-TTCTTGGGTGGCTAGGGGATA-3′; 35SF: 5′-CAGAACTC GCCGTGAAGACT-3′, 35SR: 5′-CGGCAGAGGCAGATCTTGAA-3′) (Table S1). Genomic DNA was extracted from 100 mg of shoot tissue from seedlings using the i-genomic plant DNA extraction kit (Intron Biotechnology), following the manufacturer's instructions.

Classification of transgenic T1 lines

T1 *Ppc3* lines selected (A–N) were classified depending on the degree of Sb*PPC3* silencing, *Ppc3-1* being the line with the highest degree of silencing (over 90%) and *Ppc3-14* being the line with the lowest degree (0%) (Figure S9). For classification, qPCR analysis of Sb*PPC3* transcript abundance was carried out as described in Arias-Baldrich et al. (2017), using *actin* as standard. Confirmed transgenic T1 lines were self-fertilized and homozygous T2 lines were selected for the subsequent analyses. Panicles were covered with paper bags to block cross-fertilization between *Ppc3* lines. All plants used in this work were confirmed by herbicide application and PCR, as described above in the selection of transformed *Ppc3* plants section.

Enzyme extraction and analysis

Protein extracts for PEPC activity analysis, SDS-PAGE, and immunoblot analysis were obtained by grinding 0.2 g or 0.5 g fresh weight from leaves or roots, respectively, in 1 ml of extraction buffer containing 0.1 M Tris–HCl pH 7.5, 5% (v/v) glycerol, 1 mM EDTA, 10 mM $MgCl_2$, 1 mM phenylmethylsulfonyl fluoride, 10 μg ml^{-1} chymostatin, 10 μM leupeptin, and 14 mM β-mercaptoethanol. The homogenate was centrifuged at 17 000 *g* for 5 min at 4°C, and the supernatant was used for determination of enzymatic activities.

PEPC activity was measured spectrophotometrically at pH 8 and 2.5 mM PEP as described in Echevarría et al. (1994). A single enzyme unit (U) is defined as the amount of PEPC that catalyzes the carboxylation of 1 μmol of phosphoenolpyruvate per minute at pH 8, 30°C.

For the other enzymatic activities, aliquots of 100 mg of frozen leaf or root powder were extracted in 1 ml of extraction buffer as described in Vega-Mas et al. (2019). Enzyme activities were determined by spectrophotometric methods in a 96-well microplate reader. Assays to measure CS, AAT, GDH, GS, ICDH, MDH, NR, NAD-ME, GOGAT, and NADP-ME activities were performed following Vega-Mas et al. (2019), and PK activity was measured as described in Gibon et al. (2004). For NR, 4 mM $NiCl_2$ was added to the extraction buffer to avoid interference with cyanogenic glucosides present in sorghum leaves (Maranville, 1970).

Electrophoresis and immunoblot analysis

Protein samples were denatured by heating in the presence of loading buffer (100 mM Tris–HCl, pH 8, 25% [v/v] glycerol, 1% [w/v] SDS, 10% [v/v] β-mercaptoethanol, and 0.05% [w/v] bromophenol blue). Denatured proteins (10 μg for leaf extracts and 50 μg for root extracts) were separated by SDS-PAGE in a Mini-Protean® III-2D Cell (Bio-Rad, Hercules, CA, USA) and electroblotted onto a PVDF or nitrocellulose membrane in a semidry transfer blot system (Bio-Rad). Polyclonal antibodies against native C_4-photosynthetic PEPC from sorghum leaves (anti-C_4 PTPC) were prepared as described in

Pacquit et al. (1995). These antibodies recognize both photosynthetic and non-photosynthetic PEPCs (Ruiz-Ballesta et al., 2016). Immunolabeled proteins were detected by a chemiluminescence detection system (SuperSignal West Pico Rabbit IgGs; Thermo Scientific, Waltham, MA, USA) according to the manufacturer's instructions in an Amersham Imager 600 (GE-Healthcare, Chicago, IL, USA). The signal intensities were quantified using Image Studio™ Lite software (LI-COR, Lincoln, NE, USA).

Protein quantification

Protein concentrations were determined using the method of Bradford (1976) with BSA as standard.

Gas exchange measurements

A and g_s were determined in the youngest fully developed leaf at 350 μmol m^{-2} sec^{-1} PAR, a CO_2 concentration of 400 ppm, and ambient relative humidity, using an LI-6400XT portable photosynthesis analyzer (LI-COR). The iWUE was estimated as the ratio of A to g_s (Bheemanahalli et al., 2021).

RNA extraction and cDNA synthesis

Total RNA was extracted from 100 mg of frozen powdered leaves or roots using the RNeasy Plant Mini kit (Qiagen, Hilden, Germany). Extracted nucleic acids were treated with DNase to remove genomic DNA. The RNA concentration was determined using a Nanodrop 2000 (Thermo). Reverse transcription reactions were performed using 1 μg of purified total RNA and the Transcriptor First Strand cDNA Synthesis Kit (Roche, Basel, Switzerland), following the manufacturer's instructions. cDNA synthesized was used for qPCR experiments.

Quantitative real-time PCR

qPCR reactions were performed in a final volume of 20 μl containing 1 μl of cDNA, 15 μM of specific primers (Table S1), and 10 μl of SensiFAST SYBR No-ROX kit (Bioline, Cincinnati, OH, USA). PCR was conducted on a Light Cycler 480 II Real-Time PCR System (Roche), and the cycle threshold (Ct) values were determined using Light Cycler 480 software. To normalize the obtained values, *actin* was used as internal control. Relative gene expression was calculated using the Livak method ($2^{-\Delta\Delta Ct}$; Livak & Schmittgen, 2001), with normalization to WT leaves in control conditions.

Metabolomic analysis

Central metabolites (sugars, amino acids, and organic acids) from sorghum leaves or roots were analyzed by GC-MS at the Mass Spectrometry Services (CITIUS, University of Sevilla). WT and *Ppc3-1* plants were hydroponically grown, and leaves and root tissues were collected, lyophilized, and ground in liquid nitrogen prior to GC-MS analysis. Each sample was composed of tissue from three different plants growing within the same pot. Metabolites were extracted by adding 1 ml of methanol:water (70/30, v/v) to 30 mg lyophilized leaf or root tissue. Samples were centrifuged at 13 500 ***g*** for 10 min at 4°C, and 800 μl of supernatant was stored at −80°C until use. Samples were derivatized by methoxilation with methoxilamine in 20 mg ml^{-1} pyridine (1 h, 40°C) and then trimethylsilylated with *N*-methyl-*N*-(trimethylsilyl) trifluoroacetamide (1 h, 40°C), according to the method described by Cerdán-Calero et al. (2012). The derivatives were further analyzed by GC-MS. Each sample was analyzed twice.

GC-MS was performed with a triple quadrupole mass spectrometer coupled to a TSQ8000 gas chromatograph (Thermo Scientific) equipped with a ZB-5 MS column (30 m × 0.25 mm). The temperature program for separating the MEOX-trimethylsilylated derivatives was isothermal at 70°C for 5 min, followed by a 4°C min^{-1} gradient up to 325°C. The ionization potential was 70 eV.

Metabolites were identified by the use of standards and analyzed by Automated Mass Spectral Deconvolution and Identification System (AMDIS) software (http://chemdata.nist.gov/mass-spc/amdis/downloads). Metabolites were quantified using the Qual Browser of the Xcalibur data system (Thermo).

Statistical analysis

PCA and metabolomic heatmap analysis (Figure 7) were performed using the FactoMineR (Lê et al., 2008) and Heatmap3 (Zhao et al., 2014) packages, respectively. Variable scaling was performed by dividing the centered variable by the quadratic mean using the scale function of the R vegan package.

Data were analyzed by the *t*-test or by ANOVA and means were compared by Duncan's multiple range test, as indicated in figure legends. A *P*-value of <0.05 was considered to be statistically significant. All analyses were conducted using SPSS 25 (IBM).

ACKNOWLEDGMENTS

The authors thank William Plaxton for critically reading the manuscript. We acknowledge Enrique Maguilla and Tadeo Sánchez for helping with growing and harvesting of *Ppc3* plants. We also thank Maria Eugenia Soria and Rocío Valderrama (Servicio de Espectrometría de Masas 'Centro de Investigación, Tecnología e Innovación' [CITIUS] of the University of Seville) for providing technical assistance with GC-MS analysis. We finally thank Dr. Zhanyuan Zhang and Hyeyoung Lee from the Plant Transformation Core Facility, University of Missouri, for advice on selection of transformed *Ppc3* plants. This research was supported by the Junta de Andalucía (P12-FQM-489 and PAI group BIO298), the Basque Government (IT932-16), and the Ministerio de Economía, Industria y Competitividad (AGL2012-35708 and AGL2016-75413-P).

AUTHOR CONTRIBUTIONS

CdlO performed most experiments. CdlO, JPL, ABF, GB, and JG selected transformed plants, obtained the *Ppc3-1* and *Ppc3-2* homozygous lines, harvested plants, and measured PEPC activity. CdlO and JPL analyzed GC-MS data. DM and IC measured enzymatic activities, except for PEPC. FPM obtained the pFGC161-PPC3 plasmid for sorghum transformation. JG conducted the statistical analysis of data. CE, SGM, and JAM designed the research. JAM wrote the paper with support of CE and SGM.

CONFLICT OF INTEREST

The authors have no conflict of interest to declare.

DATA AVAILABILITY STATEMENT

All relevant data can be found within the manuscript and its supporting materials.

SUPPORTING INFORMATION

Additional Supporting Information may be found in the online version of this article.

Figure S1. Relative transcript abundance of Sb*PPC1* and Sb*PPC2*.

Figure S2. Effect of salt stress on Sb*PPC3* transcript abundance, PEPC activity, and PEPC protein levels in leaves from WT or *Ppc3* plants.

Figure S3. PCA of detected primary metabolites in sorghum leaves and roots of WT or *Ppc3-1* plants under control or salt stress conditions.

Figure S4. Enzymatic activities related to C metabolism.

Figure S5. Enzymatic activities related to N metabolism.

Figure S6. Plasmid construction for Sb*PPC3* silencing in sorghum plants.

Figure S7. Selection of transformed plants.

Figure S8. Classification of T1 *Ppc3* lines by the degree of Sb*PPC3* silencing.

Figure S9. Nucleotide sequence of Sb*PPC3* and the sequence selected for silencing.

Table S1. List of primers used in this work.

REFERENCES

Álvarez, R., Gandullo, J., Feria, A.B., Dever, L.V., Vidal, J. & Echevarría, C. (2011) Characterisation of seeds of a C_4 phosphoenolpyruvatecarboxylase-deficient mutant of *Amaranthus edulis*. *Plant Biology*, **13**, 16–21.

Arias-Baldrich, C., Bosch, N., Begines, D., Feria, A.B., Monreal, J.A. & García-Mauriño, S. (2015) Proline synthesis in barley under iron deficiency and salinity. *Journal of Plant Physiology*, **183**, 121–129.

Arias-Baldrich, C., de la Osa, C., Bosch, N., Ruiz-Ballesta, I., Monreal, J.A. & García-Mauriño, S. (2017) Enzymatic activity, gene expression and post-translational modifications of photosynthetic and non-photosynthetic phosphoenolpyruvate carboxylase in ammonium-stressed sorghum plants. *Journal of Plant Physiology*, **214**, 39–47.

Baena, G., Feria, A.B., Echevarría, C., Monreal, J.A. & García-Mauriño, S. (2017) Salinity promotes opposite patterns of carbonylation and nitrosylation of C_4 phosphoenolpyruvate carboxylase in sorghum leaves. *Planta*, **246**, 1203–1214.

Bandehagh, A. & Taylor, N.L. (2020) Can alternative metabolic pathways and shunts overcome salinity induced inhibition of central carbon metabolism in crops? *Frontiers in Plant Sciences*, **11**, 1072.

Bates, G.W., Rosenthal, D.M., Sun, J., Chattopadhyay, M., Peffer, E., Yang, J. *et al.* (2012) A comparative study of the Arabidopsis thaliana guard-cell transcriptome and its modulation by sucrose. *PLoS One*, **7**(11), e49641. https://doi.org/10.1371/journal.pone.0049641

Bheemanahalli, R., Wang, C., Bashir, E., Chiluwal, A., Pokharel, M., Perumal, R. *et al.* (2021) Classical phenotyping and deep learning concur on genetic control of stomatal density and area in sorghum. *Plant Physiology*, **186**, 1562–1579.

Boxall, S.F., Kadu, N., Dever, L.V., Kneřová, J., Waller, J.L., Gould, P.D. *et al.* (2020) *Kalanchoë* PPC1 is essential for Crassulacean acid metabolism and the regulation of core circadian clock and guard cell signaling genes. *Plant Cell*, **32**(4), 1136–1160.

Bradford, M.M. (1976) A rapid and sensitive method for the quantitation of microgram quantities of protein utilizing the principle of protein-dye binding. *Analytical Biochemistry*, **72**, 248–254.

Cerdán-Calero, M., Sendra, J.M. & Sentandreu, E. (2012) Gas chromatography coupled to mass spectrometry analysis of volatiles, sugars, organic acids and aminoacids in Valencia late orange juice and reliability of the automated mass spectral deconvolution and identification system for their automatic identification and quantification. *Journal of Chromatography A*, **1241**, 84–95.

Chen, M., Yang, Z., Liu, J., Zhu, T., Wei, X., Fan, H. *et al.* (2018) Adaptation mechanism of salt excluders under saline conditions and its applications. *International Journal of Molecular Science*, **19**, 3668.

Chen, Z.H., Nimmo, G.A., Jenkins, G.I. & Nimmo, H.G. (2007) BHLH32 modulates several biochemical and morphological processes that respond to pi starvation in Arabidopsis. *Biochemical Journal*, **405**, 191–198.

Che-Othman, M.H., Millar, A.H. & Taylor, N.L. (2017) Connecting salt stress signalling pathways with salinity-induced changes in mitochondrial metabolic processes in C3 plants. *Plant, Cell & Environment*, **40**, 2875–2905.

Chollet, R., Vidal, J. & O'Leary, M. (1996) Phosphoenolpyruvate carboxylase: a ubiquitous highly regulated enzyme in plants. *Annual Review of Plant Physiology and Plant Molecular Biology*, **47**, 273–298.

Crecelius, F., Streb, P. & Feierabend, J. (2003) Malate metabolism and reactions of oxidoreduction in cold-hardened winter rye (*Secale cereale* L.) leaves. *Journal of Experimental Botany*, **54**, 1075–1083.

Dever, L.V., Blackwell, R.D., Fullwood, N.J., Lacuesta, M., Leegood, R.C., Onek, L.A. *et al.* (1995) The isolation and characterization of mutants of the C4 photosynthetic pathway. *Journal of Experimental Botany*, **46**, 1363–1376.

Dizengremel, P., Le Thiec, D., Hasenfratz-Sauder, M.P., Vaultier, M.N., Bagard, M. & Jolivet, Y. (2009) Metabolic-dependent changes in plant cell redox power after ozone exposure. *Plant Biology*, **11**, 35–42.

Do, P.T., Lee, H., Mookkan, M., Folk, W.R. & Zhang, Z.J. (2016) Rapid and efficient agrobacterium-mediated transformation of sorghum (*Sorghum bicolor*) employing standard binary vectors and bar gene as a selectable marker. *Plant Cell Reports*, **35**, 2065–2076.

Do, P.T., Lee, H., Nelson-Vasilchik, K., Kausch, A. & Zhang, Z.J. (2018) Rapid and efficient genetic transformation of sorghum via agrobacterium-mediated method. *Current Protocols in Plant Biology*, **3**, e20077.

Doubnerová, V. & Ryšlavá, H. (2011) What can enzymes of C_4 photosynthesis do for C_3 plants under stress? *Plant Science*, **180**, 575–583.

Echevarría, C., García-Mauriño, S., Álvarez, R., Soler, A. & Vidal, J. (2001) Salt stress increases the Ca^{2+}-independent phosphoenolpyruvate carboxylase kinase activity in *sorghum* leaves. *Planta*, **214**, 283–287.

Echevarría, C., Pacquit, V., Bakrim, N., Osuna, L., Delgado, B., Arrio-Dupont, M. *et al.* (1994) The effect of pH on the covalent and metabolic control of C_4 phosphoenolpyruvate carboxylase from *sorghum* leaf. *Archives of Biochemistry and Biophysics*, **315**, 425–430.

Echevarría, C. & Vidal, J. (2003) The unique phosphoenolpyruvate carboxylase kinase. *Plant Physiology and Biochemistry*, **41**, 541–547.

Ermolayev, V., Weschke, W. & Manteuffel, R. (2003) Comparison of Al-induced gene expression in sensitive and tolerant soybean cultivars. *Journal of Experimental Botany*, **54**, 2745–2756.

Feria, A.B., Bosch, N., Sánchez, A., Nieto-Ingelmo, A.I., de la Osa, C., Echevarría, C. *et al.* (2016) Phosphoenolpyruvate carboxylase (PEPC) and PEPC-kinase (PEPC-k) isoenzymes in *Arabidopsis thaliana*: role in control and abiotic stress conditions. *Planta*, **244**, 901–913.

Gandullo, J., Álvarez, R., Feria, A.B., Monreal, J.A., Díaz, I., Vidal, J. *et al.* (2021) A conserved C-terminal peptide of sorghum phosphoenolpyruvate carboxylase promotes its proteolysis, which is prevented by Glc-6P or the phosphorylation state of the enzyme. *Planta*, **254**, 43.

Gandullo, J., Monreal, J.A., Álvarez, R., Díaz, I., García-Mauriño, S. & Echevarría, C. (2019) Anionic phospholipids induce conformational changes in phosphoenolpyruvate carboxylase to increase sensitivity to cathepsin proteases. *Frontiers in Plant Science*, **10**, 582.

García-Mauriño, S., Monreal, J.A., Álvarez, R., Vidal, J. & Echevarría, C. (2003) Characterization of salt stress-enhanced phosphoenolpyruvate carboxylase kinase activity in leaves of *Sorghum vulgare*: independence from osmotic stress, involvement of ion toxicity and significance of dark phosphorylation. *Planta*, **216**, 648–655.

Gasparis, S., Orczyk, W., Zalewski, W. & Nadolska-Orczyk, A. (2011) The RNA-mediated silencing of one of the pin genes in allohexaploid wheat simultaneously decreases the expression of the other, and increases grain hardness. *Journal of Experimental Botany*, **62**, 4025–4036.

Gibon, Y., Blaesing, O.E., Hannemann, J., Carillo, P., Höhne, M., Hendriks, J.H. *et al.* (2004) A robot-based platformto measure multiple enzyme activities in Arabidopsis using a set of cyclingassays: comparison of changes of enzyme activities and transcriptlevels during diurnal cycles and in prolonged darkness. *The Plant Cell*, **16**, 3304–3325.

González, M.C., Sánchez, R. & Cejudo, F.J. (2003) Abiotic stresses affecting water balance induce phosphoenolpyruvate carboxylase expression in roots of wheat seedlings. *Planta*, **216**, 985–992.

Gregory, A.L., Hurley, B.A., Tran, H.T., Valentine, A.J., She, Y.M., Knowles, V.L. *et al.* (2009) *In vivo* regulatory phosphorylation of the phosphoenolpyruvate carboxylase AtPPC1 in phosphate-starved *Arabidopsis thaliana*. *Biochemical Journal*, **420**, 57–65.

Hasegawa, P.M., Bressan, R.A., Zhu, J.K. & Bohnert, H.J. (2000) Plant cellular and molecular responses to high salinity. *Annual Review of Plant Physiology and Plant Molecular Biology*, **51**, 463–499.

Herrera-Rodríguez, M.B., Pérez-Vicente, R. & Maldonado, J.M. (2007) Expression of asparagine synthetase genes in sunflower (*Helianthus annuus*) under various environmental stresses. *Plant Physiology and Biochemistry*, **45**, 33–38.

Hewitt EJ. 1966. Sand and water culture methods used in the study of plant nutrition. Commonwealth Bureau of Horticultural and Plantation Crops, East Malling Technology Communications No. 22.

Huppe, H.C. & Turpin, D.H. (1994) Integration of carbon and nitrogen metabolism in plant and algal cells. *Annual Review of Plant Physiology and Plant Molecular Biology*, **45**, 577–607.

Kanai, R. & Edwards, G.E. (1999) The biochemistry of C_4 photosynthesis. In: Sage, R.F. & Monson, R.K. (Eds.) *C_4 plant biology*. San Diego, CA: Academic Press, pp. 49–87.

Lamers, J., van der Meer, T. & Testerink, C. (2020) How plants sense and respond to stressful environments. *Plant Physiology*, **182**, 1624–1635.

Lasa, B., Frechilla, S., Aparicio-Tejo, P.M. & Lamsfus, C. (2002) Role of glutamate dehydrogenase and phosphoenolpyruvate carboxylase activity in ammonium nutrition tolerance in roots. *Plant Physiology and Biochemistry*, **40**, 969–976.

Lê, S., Josse, J. & François, H. (2008) FactoMineR: an R package for multivariateanalysis. *Journal of Statistical Software*, **25**, 1–18.

Lea, P.J. (1997) Primary nitrogen metabolism. In: Dey, P.M. & Harborne, J.B. (Eds.) *Plant biochemistry*. London, UK: Academic Press, pp. 273–306.

Lepiniec, L., Thomas, M. & Vidal, J. (2003) From enzyme activity to plant biotechnology: 30 years of research on phosphoenolpyruvate carboxylase. *Plant Physiology and Biochemistry*, **41**, 533–539.

Liang, X., Liu, S., Wang, T., Li, F., Cheng, J., Lai, J. *et al.* (2021) Metabolomics-driven gene mining and genetic improvement of tolerance to salt-induced osmotic stress in maize. *New Phytologist*, **230**, 2355–2370.

Livak, K.J. & Schmittgen, T.D. (2001) Analysis of relative gene expression data using real-time quantitative PCR and the $2^{-\Delta\Delta Ct}$ method. *Methods*, **25**, 402–408.

López-Millán, A.F., Morales, F., Andaluz, S., Gogorcena, Y., Abadía, A., de las Rivas, J. *et al.* (2000) Responses of sugar beet roots to iron deficiency. Changes in carbon assimilation and oxygen use. *Plant Physiology*, **124**, 885–898.

Ma, N.L., Che Lah, W.A., Abd Kadir, N., Mustaqim, M., Rahmat, Z., Ahmad, A. *et al.* (2018) Susceptibility and tolerance of rice crop to salt threat: physiological and metabolic inspections. *PLoS One*, **13**, e0192732.

Mansour, M.M. (2000) Nitrogen containing compounds and adaptation of plants to salinity stress. *Biologia Plantarum*, **43**, 491–500.

Mansour, M.M., Emam, M.M., Salama, K.H.A. & Morsy, A.A. (2021) Sorghum under saline conditions: responses, tolerance mechanisms, and management strategies. *Planta*, **254**, 24.

Maranville, J.W. (1970) Influence of nickel on the detection of nitrate reductase activity in sorghum extracts. *Plant Physiology*, **45**, 591–593.

Monreal, J.A., Feria, A.B., Vinardell, J.M., Vidal, J., Echevarría, C. & García-Mauriño, S. (2007a) ABA modulates the degradation of phospho*enol*pyruvate carboxylase kinase in sorghum leaves. *FEBS Letters*, **581**, 3468–3472.

Monreal, J.A., López-Baena, F.J., Vidal, J., Echevarría, C. & García-Mauriño, S. (2007b) Effect of LiCl on phosphoenolpyruvate carboxylase kinase and the phosphorylation of phosphoenolpyruvate carboxylase in leaf disks and leaves of *Sorghum vulgare*. *Planta*, **225**, 801–812.

Monreal, J.A., McLoughlin, F., Echevarría, C., García-Mauriño, S. & Testerink, C. (2010) Phospho*enol*pyruvate carboxylase from C_4 leaves is selectively targeted for inhibition by anionic phospholipids. *Plant Physiology*, **152**, 634–638.

Munns, R. (2002) Comparative physiology of salt and water stress. *Plant, Cell & Environment*, **25**, 239–250.

Munns, R. & Tester, M. (2008) Mechanisms of salinity tolerance. *Annual Review of Plant Biology*, **59**, 651–681.

Nocito, F.F., Espen, L., Crema, B., Cocucci, M. & Sacchi, G.A. (2008) Cadmium induces acidosis in maize root cells. *New Phytologist*, **179**, 700–711.

O'Leary, B., Asao, S., Millar, A.H. & Atkin, O.K. (2019) Core principles which explain variation in respiration across biological scales. *New Phytologist*, **222**, 670–686.

O'Leary, B., Park, J. & Plaxton, W.C. (2011) The remarkable diversity of plant PEPC (phosphoenolpyruvate carboxylase): recent insights into the physiological functions and post-translational controls of non-photosynthetic PEPCs. *Biochemical Journal*, **436**, 15–34.

O'Leary, B., Rao, S.K., Kim, J. & Plaxton, W.C. (2009) Bacterial-type phosphoenolpyruvate carboxylase (PEPC) functions as a catalytic and regulatory subunit of the novel class-2 PEPC complex of vascular plants. *Journal of Biological Chemistry*, **284**, 24797–24805.

Outlaw, W.H. (1990) Kinetic properties of guard-cell phosphoenolpyruvate carboxylase. *Biochemie und Physiologie der Pflanzen*, **186**, 317–325.

Pacquit, V., Giglioli, N., Crétin, C., Pierre, J.N., Vidal, J. & Echevarría, C. (1995) Regulatory phosphorylation of C4 phosphoenolpyruvate carboxylase from Sorghum: an immunological study using specific anti-phosphorylation site-antibodies. *Photosynthesis Research*, **43**, 283–288.

Park, J., Khuu, N., Howard, A.S.M., Mullen, R.T. & Plaxton, W.C. (2012) Bacterial- and plant-type phosphoenolpyruvate carboxylase isozymes from developing castor oil seeds interact *in vivo* and associate with the surface of mitochondria. *The Plant Journal*, **71**, 251–262.

Paterson, A.H., Bowers, J.E., Bruggmann, R., Dubchak, I., Grimwood, J., Gundlach, H. *et al.* (2009) The *Sorghum bicolor* genome and the diversification of grasses. *Nature*, **457**, 551–556.

Rashmi, D., Barvkar, V.T., Nadaf, A., Mundhe, S. & Kadoo, N.Y. (2019) Integrative omics analysis in *Pandanus odorifer* (Forssk.) Kuntze reveals the role of asparagine synthetase in salinity tolerance. *Scientific Reports*, **9**, 932.

Ruiz-Ballesta, I., Baena, G., Gandullo, J., Wang, L., She, Y.M., Plaxton, W.C. *et al.* (2016) New insights into the post-translational modification of multiple phosphoenolpyruvate carboxylase isoenzymes by phosphorylation and monoubiquitination during sorghum seed development and germination. *Journal of Experimental Botany*, **67**, 3523–3536.

Ruiz-Ballesta, I., Feria, A.B., Ni, H., She, Y.M., Plaxton, W.C. & Echevarría, C. (2014) *In vivo* monoubiquitination of anaplerotic phosphoenolpyruvate carboxylase occurs at Lys624 in germinating sorghum seeds. *Journal of Experimental Botany*, **65**, 443–451.

Sage, R.F., Sage, T.L. & Kocacinar, F. (2012) Photorespiration and the evolution of C_4 photosynthesis. *Annual Review of Plant Biology*, **63**, 19–47.

Sánchez, D.H., Siahpoosh, M.R., Roessner, U., Udvardi, M. & Kopka, J. (2008) Plant metabolomics reveals conserved and divergent metabolic responses to salinity. *Physiologia Plantarum*, **132**, 209–219.

Shenton, M., Fontaine, V., Hartwell, J., Marsh, J.T., Jenkins, G.I. & Nimmo, H.G. (2006) Distinct patterns of control and expression amongst members of the PEP carboxylase kinase gene family in C_4 plants. *The Plant Journal*, **48**, 45–53.

Shi, J., Yi, K., Liu, Y., Xie, L., Zhou, Z., Chen, Y. *et al.* (2015) Phosphoenolpyruvate carboxylase in Arabidopsis leaves plays a crucial role in carbon and nitrogen metabolism. *Plant Physiology*, **167**, 671–681.

Sweetlove, L.J., Beard, K.F.M., Nunes-Nesi, A., Fernie, A.R. & Ratcliffe, R.G. (2010) Not just a circle: flux modes in the plant TCA cycle. *Trends in Plant Science*, **15**, 462–470.

Taiz, L., Zeiger, E., Møller, I.M. & Murphy, A. (2018) *Plant physiology and development*. Sunderland: Sinauer Associates, pp. 745–747 (ISBN 978–1–60535-255-8).

Takahashi-Terada, A., Kotera, M., Ohshima, K., Furumoto, T., Matsumura, H., Kai, Y. *et al.* (2005) Maize phosphoenolpyruvate carboxylase. Mutations at the putative binding site for glucose 6-phosphate caused desensitization and abolished responsiveness to regulatory phosphorylation. *Journal of Biological Chemistry*, **280**, 11798–11806.

Toyota, K., Koizumi, N. & Sato, F. (2003) Transcriptional activation of phosphoenolpyruvate carboxylase by phosphorus deficiency in tobacco. *Journal of Experimental Botany*, **54**, 961–969.

Ushakova, S.A., Kovaleva, N.P., Tikhomirova, N.A., Gribovskaya, I.V. & Kolmakova, A.A. (2006) Effect of photosynthetically active radiation, salinization, and type ofnitrogen nutrition on growth of *Salicornia europaea*. *Russian Journal of Plant Physiology*, **53**, 785–793.

Vega-Mas, I., Cukier, C., Coleto, I., González-Murua, C., Limami, A.M., González-Moro, M.B. *et al.* (2019) Isotopic labelling reveals the efficient adaptation of wheat root TCA cycle flux modes to match carbon demand under ammonium nutrition. *Scientific Reports*, **9**, 8925.

Wang, C.Y., Shen, R.F., Wang, C. & Wang, W. (2013) Root protein profile changes induced by Al exposure in two rice cultivars differing in Al tolerance. *Journal of Proteomics*, **78**, 281–293.

Willick, I.R., Plaxton, W.C., Lolle, S.J. & Macfie, S.M. (2019) Transcriptional and post-translational upregulation of phosphoenolpyruvate carboxylase in *Arabidopsis thaliana* (L- Heynh) under cadmium stress. *Environmental and Experimental Botany*, **164**, 29–39.

van Zelm, E., Zhang, Y. & Testerink, C. (2020) Salt tolerance mechanisms of plants. *Annual Review of Plant Biology*, **71**, 24.1–24.31.

Zhao, S., Guo, Y., Sheng, Q. & Shyr, Y. (2014) Heatmap3: an improved heatmap package with more powerful and convenient features. *BMC Bioinformatics*, **15**, P16.

Zhao, Z.-Y. & Dahlberg, J. (2019) *Sorghum: methods and protocols*. Berlin, Germany: Springer Nature.